

THE POLARIZED (d, $\alpha$ ) REACTION NEAR 0°

PARITY MEASUREMENTS  
USING  
THE POLARIZED (d,  $\alpha$ ) REACTION NEAR 0°

By

DOUGLAS THOMAS PETTY, B.Sc.

A Thesis

Submitted to the School of Graduate Studies

in Partial Fulfilment of the Requirements

for the Degree

Doctor of Philosophy

McMaster University

December 1976

AS THOMAS PETTY

DOCTOR OF PHILOSOPHY (1976)  
(Physics)

McMASTER UNIVERSITY  
Hamilton, Ontario

TITLE: Parity Measurements Using the Polarized (d, $\alpha$ ) Reaction  
Near 0°

AUTHOR: Douglas Thomas Petty, B.Sc. (University of Calgary)

SUPERVISOR: Professor John A. Kuehner

NUMBER OF PAGES: ix, 77

### Abstract

A new model-independent method is presented for determining certain spectroscopic information in odd-odd nuclei. It uses the (d, $\alpha$ ) reaction with a polarized deuteron beam incident on a spin-zero target nucleus and with the alpha particles detected near  $0^\circ$  to the beam direction. By measuring the tensor analyzing power for the reaction to a particular final state, it is possible to determine whether that state has natural parity or unnatural parity. In addition, the method allows spin-zero levels in the final nucleus to be uniquely identified and the tensor polarization of the beam to be measured. The fluctuations of the tensor analyzing power with energy for unnatural parity states are calculated using the statistical compound nucleus model and it is shown that, for most cases, an average of the cross-sections for three energies will be sufficient for unambiguously assigning natural parity or  $0^-$  to a level. It has also been shown that the expected attenuation of the tensor analyzing power for natural parity states is negligible when the alpha particles are detected near  $0^\circ$ .

This method is applied to the reactions  $^{12}\text{C}(d,\alpha)^{10}\text{B}$ ,  $^{16}\text{O}(d,\alpha)^{14}\text{N}$ , and  $^{40}\text{Ca}(d,\alpha)^{38}\text{K}$ , resulting in many new spin and parity assignments. In particular, assignments of  $J^\pi = 0^-$  are made to the 4.91 MeV level and to one member of the doublet at 9.13 MeV in  $^{14}\text{N}$ . Assignments of  $3^-$ ,  $(2,4)^-$ ,  $2^-$ ,  $(2^-,3^+)$ ,  $2^-$ ,  $1^+$ , and  $1^+$  are made to the 2613, 2647, 2870, 3317, 3815, 3857, and 3978 keV states, respectively, of  $^{38}\text{K}$ .

The results of a shell-model calculation of the negative parity  $T = 0$  states in  $^{38}\text{K}$  are presented.

### Acknowledgements

It is difficult to appropriately acknowledge all the people who influenced me in my work at McMaster but I would like, in particular, to mention the following:

John Kuehner, my supervisor, for his inspiration and encouragement at all stages in my research;

Peter Green and Graham Jones for their help during the initial (difficult) stages of this work;

Drs. J.C. Waddington and R.H. Tomlinson, the other members of my supervisory committee, for their interest;

Dave Kelly who gave to me some of his knowledge about the lab computers;

Terry Taylor for introducing me to some of the subtleties of shell-model calculations;

Past and present members of the group for their assistance and advice including Wayne Greene, Judit Szucs, Henry Weller, Pitsa Ikossi, Dik Boerma, Alex McDonald, and Bruce Wilkin;

John McKay for his achievements in the operation of the polarized ion source and for graciously answering his telephone if we had problems at 3 o'clock in the morning;

My wife, Patti; for preparing most of the drawings and typing the final manuscript and especially for her patience;

and the National Research Council of Canada for providing financial assistance in the form of postgraduate scholarships.

E

TABLE OF CONTENTS

<u>CHAPTER</u>		<u>Page</u>
	INTRODUCTION	1
I	POLARIZATION IN NUCLEAR REACTIONS	
	Introduction	7
	Specification of the Polarization of a System	8
	Analyzing Powers - Cross-sections	14
II	THE (d, $\alpha$ ) REACTION NEAR 0°	
	Introduction	18
	T <sub>20</sub> for Natural Parity and 0 <sup>-</sup> States	18
	Unnatural Parity States - Ericson Fluctuations	20
	Deviations from 0° - Compound Statistical Model	27
III	THE <sup>12</sup> C(d, $\alpha$ ) <sup>10</sup> B AND <sup>16</sup> O(d, $\alpha$ ) <sup>14</sup> N EXPERIMENTS	
	Introduction	31
	Experimental Details	32
	The <sup>12</sup> C(d, $\alpha$ ) <sup>10</sup> B Reaction	38
	The <sup>16</sup> O(d, $\alpha$ ) <sup>14</sup> N Reaction	42
IV	THE <sup>40</sup> Ca(d, $\alpha$ ) <sup>38</sup> K EXPERIMENT	
	Introduction	50
	Procedure	50
	Results	51

(continued)

TABLE OF CONTENTS (continued)

<u>CHAPTER</u>		<u>Page</u>
V	SHELL MODEL CALCULATIONS FOR $^{38}\text{K}$	
	Introduction	59
	Details of the Calculation	59
	Results	64
	CONCLUSIONS	71

LIST OF FIGURES

<u>FIGURE</u>		<u>Page</u>
2.1	Distribution of tensor analyzing power for unnatural parity states for different values of N.	24
2.2	Distribution of tensor analyzing power for unnatural parity states for different amplitude ratios.	25
2.3	Calculated angular distribution of tensor analyzing power for natural parity state.	29
3.1	General beam line layout.	33
3.2	Target chamber setup.	36
3.3	Proportional counter schematic.	37
3.4	Electronics setup.	39
3.5	Spectra from the $^{12}\text{C}(d,\alpha)^{10}\text{B}$ reaction.	40
3.6	Experimental angular distribution of tensor analyzing power for 3.59 MeV, $2^+$ state in $^{10}\text{B}$ .	43
3.7	Spectra from the $^{16}\text{O}(d,\alpha)^{14}\text{N}$ reaction.	45
3.8	Tensor analyzing power for states from the $^{16}\text{O}(d,\alpha)^{14}\text{N}$ reaction.	46
3.9	Tensor analyzing power for states from the $^{12}\text{C}(d,\alpha)^{10}\text{B}$ reaction.	47
4.1	Spectra from the $^{40}\text{Ca}(d,\alpha)^{38}\text{K}$ reaction.	52
4.2	Tensor analyzing power for states from the $^{40}\text{Ca}(d,\alpha)^{38}\text{K}$ reaction from 1698 to 3458 keV.	53
4.3	Tensor analyzing power for states from the $^{40}\text{Ca}(d,\alpha)^{38}\text{K}$ reaction from 3615 to 3978 keV.	54
5.1	$^{38}\text{Ar} - ^{38}\text{K}$ level diagram.	60
5.2	Shell structure around $^{38}\text{K}$	62
5.3	Calculated T = 0 negative parity states.	66

(continued)



LIST OF FIGURES (continued)

<u>FIGURE</u>		<u>Page</u>
5.4	Calculated level energies as a function of the MSDI parameter $A_0$ .	68
5.5	Calculated level energies as a function of the MSDI parameter $A_1$ .	69

LIST OF TABLES

<u>TABLE</u>		<u>Page</u>
1.1	Spherical tensor operators for $s = 1/2$ and $s = 1$ .	10
1.2	Relationship between spherical tensor operators and angular momentum operators.	12
2.1	Values of the cumulative probability for various deviations from the limits of $T_{20}$ .	26
2.2	Calculated attenuation of the tensor analyzing power for natural parity states when detecting the alpha particles slightly off axis.	30
3.1	Vector and tensor polarization for the three deuteron magnetic substates.	35
3.2	Calculation of tensor analyzing power and fractional beam polarization from yield ratios.	41
4.1	$\langle T_{20} \rangle$ for $^{40}\text{Ca}(d,\alpha)^{38}\text{K}$ reaction.	55
5.1	Parameters used in the shell model calculation.	65
5.2	Dominant configurations in some low-lying negative parity states.	70

## INTRODUCTION

A major goal of nuclear physics is to understand the structure of the atomic nucleus and the forces which hold it together. In this quest for understanding, a great deal of progress has been made and the properties of many hundreds of nuclei explored. Since most nuclei contain several nucleons\* the mathematical problem of solving the resulting many-body equations is intractable. This is one reason that various models have been proposed to try and explain the gross structure of nuclei and some of these have had a surprising amount of success despite their simplicity. These models differ widely in their approach to the nuclear problem and often apply to only a specific class of nuclei, however they all have two things in common: they attempt to explain the known properties of nuclei and they predict properties which have not yet been measured experimentally. When (and if) a model is found which satisfactorily "explains" all the known properties of nuclei in terms of basic forces and microscopic structure, then a major goal of nuclear physics will have been reached.

The importance of spectroscopic information in the scientific process is clear -in the beginning it provides the initial impetus for formulating a model of nuclear structure; later, it allows a choice to be made concerning the suitability of a particular model and provides

---

\*The generic term for neutrons and protons.

guidelines for refinements in that model. Since the amount of information that one can obtain about any given nucleus is enormous, a judicious selection will be necessary. To some extent, however, nature has made the choice for us. We are constrained in our study by the current state of the art in technology (and ideas). There are some properties of nuclei which are beyond our grasp at the present time because of limitations in our experimental techniques or technology and, in fact, many of the advances in modern technology can be seen to arise, directly or indirectly, from the needs of the nuclear physicist.

And just what are the properties of a nucleus that we are interested in and capable of measuring? Typically the first properties to be measured are the energies that a particular nucleus is allowed to have.\* These, along with the spin and parity of the state, its dipole, quadrupole and possibly higher-order moments and its deformation are some of the static properties of the nucleus. In contrast, the type and rate of transitions between states may be thought of as the dynamic properties of the system. The lowest or ground state of the nucleus can often be studied with the techniques of atomic beam spectroscopy whereas excited states are usually studied using nuclear reactions. In both cases, a host of methods has evolved for determining the characteristics of these states (Segré, 1953; Gove and Robinson, 1966; and England, 1974). In a discussion of any nuclear technique, there are three overriding considerations: its applicability, its reliability and its simplicity. The importance of the first and last points are obvious.

---

\*These are called energy levels or states.

The question of reliability is another matter. Obviously, if someone makes a measurement using a particular technique and claims some result, the physics community (or the experimenter himself) should somehow decide how reliable is the result. This is difficult however, since many methods rely on assumptions about the basic reaction mechanism\* and therefore the question of reliability is often intimately connected with the methods applicability. From this discussion it should be clear that any method that is model-independent is to be preferred over one which is not.

With the advent of polarized beams, the opportunity now exists for new types of experiments to yield spectroscopic information. In this thesis a new method of parity determination is presented and developed. The method is model-independent and relies on only the conservation laws of angular momentum and parity and can be applied to states in odd-odd nuclei (i.e. nuclei with an odd number of protons and an odd number of neutrons) with the only restriction being on the energy resolution of the system. Basically one can determine if a state has natural ( $\pi = (-1)^J$ ) or unnatural ( $\pi = (-1)^{J+1}$ ) parity (where  $J$  is the spin of the state and  $\pi$  the parity). This allows the parity of a state to be determined if the spin is known and the spin to be determined in some cases if there is sufficient previous information on the possible spin-parity combinations of the state. There are three basic conditions which must be satisfied in order that the above selection rule is valid: (1) the target nucleus must have a ground state spin and parity of  $0^+$ ; (2) the incident beam must have  $J^\pi = 1^+$  which of course applies to deuterons but also applies to  ${}^6\text{Li}$  beams as well, and; (3) the alpha particles (or any  $J^\pi = 0^+$  outgoing particles) from the

---

\* We will call these methods model-dependent.

reaction must be detected at  $0^\circ$  or  $180^\circ$  to the beam direction. Since all even-even nuclei have  $J^\pi = 0^+$  it is easy to see from condition (1) why the method is used to study states in odd-odd nuclei.

To give a brief understanding of the reasons behind this selection rule, let us consider the reaction  $^{12}\text{C}(d,\alpha)^{10}\text{B}$  as an example. If we define  $\vec{l}_i$  and  $\vec{l}_f$  to be the orbital angular momenta in the initial and final channels, respectively and if we denote the spin and parity of the final state in  $^{10}\text{B}$  as  $J^\pi$  then conservation of angular momentum and parity require that

$$\vec{l}_i + \vec{1} = \vec{l}_f + \vec{J}$$

and

$$\pi = (-1)^{l_i + l_f}$$

If we take the quantization axis to be in the direction of the incident beam then the projections of both the initial and final orbital angular momenta on this axis will be zero. In addition, if the deuteron beam is polarized in its  $m = 0$  substate relative to the beam direction then the angular momentum coupling coefficients will appear in the expression for the cross section as products

$$(l_i \ 0, \ 1 \ 0 | J \ 0) (l_f \ 0, \ J \ 0 | J \ 0)$$

Since the coefficient  $(j_1 \ 0, \ j_2 \ 0 | j \ 0) \neq 0$  only if  $j_1 + j_2 + j$  is even, it is clear that the cross section can be non-zero only if  $l_i + l_f + 1 + J$  is even. Combining this with the expression for parity conservation yields the result that the cross-section can only be non-zero if  $\pi = (-1)^{J+1}$ , i.e. an unnatural parity state.

So the procedure involved in determining whether a state has natural or unnatural parity is (to compare the cross section using an  $m = 0$  deuteron beam with the cross section using an  $m \neq 0$  beam. The ratio of these cross sections will always be zero for a natural parity state but will, in general, be non-zero for an unnatural parity state. The development of these ideas, together with experimental data for states in  $^{10}\text{B}$ ,  $^{14}\text{N}$ , and  $^{38}\text{K}$  represent the major portion of this thesis.

Chapter I contains a collection of formulae and expressions for the reaction amplitudes and cross sections appropriate when dealing with polarized beams. It is necessary to introduce some new terminology since one can obtain much more information about a nucleus by studying the polarization "dependence" of nuclear reactions.

Chapter II develops the method in a rigorous way starting from the expressions contained in chapter I. In addition there are several technical points that one must consider when using a method such as this. First the effect of detecting the alpha particles slightly off axis must be determined. Even if the detector were located at  $0^\circ$  or  $180^\circ$ , the finite solid angle subtended by it would mean that some particles were detected off axis. Second, we have mentioned that the above yield ratio would be zero for a natural parity state and will usually be non-zero for an unnatural parity state. Occasionally, however, the yield ratio might be zero for an unnatural parity state for entirely different reasons and this would lead to incorrect assignments of natural parity. To overcome this problem one would usually repeat the measurement at several beam energies and if the yield ratio continued to be zero then one could be more confident of an assignment of natural parity. These

two points are dealt with at length in Chapter II. Also it will become apparent that this method can be used to uniquely identify spin-zero levels and to measure certain components of the beam polarization.

Chapter III gives a detailed discussion of the experimental technique used - that of detecting the alpha particles near  $0^\circ$  with a magnetic spectrograph. The advantages and disadvantages of this approach are outlined along with the results of the experiments  $^{12}\text{C}(d,\alpha)^{10}\text{B}$ ,  $^{16}\text{O}(d,\alpha)^{14}\text{N}$  used to demonstrate the method and determine its feasibility.

Chapter IV presents the results for the experiment  $^{40}\text{Ca}(d,\alpha)^{38}\text{K}$ . This was particularly fruitful in terms of the new spin and parity assignments that resulted but, in terms of the low cross section for the reaction and the energy resolution required by the detectors, it probably represents the practical limit for this type of experiment.

Finally, chapter V presents the results of a theoretical calculation for the energies of the low-lying negative parity states in  $^{38}\text{K}$ . The new assignments in this nucleus made a shell model calculation for these states desirable.



## CHAPTER I - Polarization in Nuclear Reactions

### Introduction

The description of nuclear reactions so as to emphasize their polarization dependence is a fairly straightforward generalization of existing formalism. Unfortunately there exist a number of conventions for the discussion of polarization effects and the presentation of experimental data, which, needless to say, greatly hinder the comparison of different work. At the Madison conference in 1970, a convention was adopted concerning the notation and coordinate systems used for describing polarization phenomena and since this has enjoyed a relatively wide acceptance among physicists working in the field, it will be used here.

In this chapter, the formalism for describing polarization phenomena will be developed and expressions for the analyzing powers given in terms of reaction amplitudes. Excellent discussions of these matters can be found in Welton (1963) and Darden (1971) although neither of these authors adhere strictly to the Madison convention. The development presented in this chapter follows closely the work of Simonius (1974). No reaction theory will be presented but only the general symmetry relationships and angular momentum coupling that all theories must include. The resulting expressions, which at first glance appear rather complicated, allow a great deal of simplification when the condition of detecting the outgoing particles at  $0^\circ$  or  $180^\circ$  is imposed. In all of what follows, we restrict ourselves to the cases where only one particle in the incident

channel and one particle in the exit channel has spin. This applies to the (d,  $\alpha$ ) reactions considered in this thesis and generalizations to cases where more than one particle in either channel have non-zero spin is straightforward.

### Specification of the Polarization of a System

Consider a particle with spin  $s$ . The spin wave function for this particle can be expressed as a linear combination of some set of basis spinors

$$|\chi\rangle = \sum_{\mu} a_{\mu} |\mu\rangle$$

where  $\mu$  is the projection of  $s$  in some, as yet unspecified, coordinate system. For a different coordinate system (labelled as II) connected to the first system by a rotation specified by the Euler angles  $R = (\alpha, \beta, \gamma)$ , the basis states will transform as

$$|\mu'\rangle_{\text{II}} = \sum_{\mu} D_{\mu\mu'}^s |\mu\rangle_{\text{I}}$$

The same state in the rotated frame can be expressed as

$$|\chi\rangle = \sum_{\mu'} a_{\mu'}^{\text{II}} |\mu'\rangle_{\text{II}} = \sum_{\mu} a_{\mu}^{\text{I}} |\mu\rangle_{\text{I}}$$

and hence

$$a_{\mu}^{\text{I}} = \sum_{\mu'} a_{\mu'}^{\text{II}} D_{\mu\mu'}^s (R) \quad [1a]$$

with the obvious inverse

$$a_{\mu'}^{\text{II}} = \sum_{\mu} a_{\mu}^{\text{I}} D_{\mu'\mu}^s (R^{-1}) \quad [1b]$$

$$= \sum_{\mu} a_{\mu}^{\dagger} D_{\mu\mu'}^{*S} (R)$$

For a system of identical particles with spin, their state can be completely described by the density matrix defined by

$$\rho_{\mu\mu'} = \langle a_{\mu} a_{\mu'}^* \rangle$$

in which the products of amplitudes  $a_{\mu} a_{\mu'}^*$  are averaged over all elements of the system. If every particle in the system has the same wavefunction then the system is said to be in a pure state and it is completely polarized, otherwise it is said to be in a mixed state. The transformation of an element of the density matrix under a rotation of the coordinate axes will now involve a product of two D-functions.

It is convenient to introduce the spherical tensor moments for describing the polarization state of a system (Lakin, 1955; Darden, 1967). They are defined by

$$\begin{aligned} t_{kq} &= \sqrt{2s+1} \sum_{\mu\mu'} (-1)^{s-\mu} (s\mu', s-\mu | kq) \rho_{\mu\mu'} \quad [2] \\ &\equiv \langle \Upsilon_{kq} \rangle \quad 0 \leq k \leq 2s \\ &= \text{Tr} (\Upsilon_{kq} \rho) \quad -k \leq q \leq k \end{aligned}$$

A list of the operators  $(\Upsilon_{kq})_{\mu\mu'}$ , for  $s = 1/2$  and  $s = 1$  is given in table 1.1.

There are several advantages for using the  $t_{kq}$  to describe the polarization of a system. They are:

Table 1.1

Spherical tensor operators for  $s = 1/2$  and  $s = 1$ 

$$(\tau_{kq})_{\mu\mu'} = \sqrt{2s+1} (-1)^{s-\mu} \langle s \mu' s -\mu | k q \rangle$$

 $s = 1/2$ 

Notation

		0 0	1 0	1 1			
					k q	k q	...
1/2	1/2	1	1	0	$\mu'$	$\mu$	
-1/2	-1/2	1	-1	0	...		
1/2	-1/2	0	0	$-\sqrt{2}$			

 $s = 1$ 

		0 0	1 0	2 0	1 1	2 1	2 2
1	1	1	$\sqrt{3/2}$	$\sqrt{1/2}$	0	0	0
0	0	1	0	$-\sqrt{2}$	0	0	0
-1	-1	1	$-\sqrt{3/2}$	$\sqrt{1/2}$	0	0	0
1	0	0	0	0	$-\sqrt{3/2}$	$-\sqrt{3/2}$	0
0	-1	0	0	0	$-\sqrt{3/2}$	$\sqrt{3/2}$	0
1	-1	0	0	0	0	0	$\sqrt{3}$

$$\begin{aligned}
 (\tau_{kq})_{\mu\mu'} &= (-1)^k (\tau_{k-q})_{-\mu'-\mu} \\
 &= (-1)^q (\tau_{k-q})_{\mu\mu'} \\
 &= (-1)^{k+q} (\tau_{kq})_{-\mu-\mu'}
 \end{aligned}$$

- (i) The transformation from one coordinate system to another is simpler for  $t_{kq}$  than for  $\rho_{\mu\mu'}$ . The analog to equation [1] is

$$t_{kq}^{\text{II}} = \sum_{q'} D_{q'q}^s t_{kq'}^{\text{I}} \quad [3]$$

- (ii) The values of  $t_{kq}$  for small values of  $k$  correspond to elementary polarization properties of the system. Table 1.2 shows the  $t_{kq}$  expressed in terms of the vector spin operators and the Pauli matrices for  $s = 1/2$  and  $s = 1$ .
- (iii) They are irreducible, i.e. the  $t_{kq}$  for a given  $k$  only transform among themselves. For  $k = 1$ , if any of the  $t_{1q}$  are non-zero then the system is said to be vector polarized and for  $k = 2$ , if any of the  $t_{2q}$  are non-zero then the system is said to be tensor polarized. Of course, it is possible for a system to have both vector and tensor polarizations but if a system has only vector polarization, say, then it will not have any tensor polarization in any coordinate reference frame.

It is useful to consider some of the symmetry relationships among the  $t_{kq}$ . Since the density matrix is hermitean, the tensor moments will be related as

$$t_{kq}^* = (-1)^q t_{k-q} \quad [4]$$

If the system is unpolarized then

$$t_{kq} = 0 \quad \text{for} \quad k, q \neq 0$$

Table 1.2

Relationship between spherical tensor operators and angular momentum operators.

$$s = 1/2$$

$$\tau_{00} = 1$$

$$\tau_{10} = \sigma_z$$

$$\tau_{1\pm 1} = \mp (1/\sqrt{2}) (\sigma_x \pm i\sigma_y)$$

$$s = 1$$

$$\tau_{00} = 1$$

$$\tau_{10} = (\sqrt{3}/2) S_z$$

$$\tau_{1\pm 1} = \mp (\sqrt{3}/2) (S_x \pm iS_y)$$

$$\tau_{20} = (1/\sqrt{2}) (3S_z^2 - 2)$$

$$\tau_{2\pm 1} = \mp (\sqrt{3}/2) [(S_x \pm iS_y)S_z + S_z(S_x \pm iS_y)]$$

$$\tau_{2\pm 2} = (\sqrt{3}/2) (S_x \pm iS_y)^2$$

If the system is axially symmetric about the z-axis then

$$t_{kq} = 0 \quad \text{for } q \neq 0$$

If the system is symmetric with respect to reflection in the x-z plane then

$$t_{kq} = (-1)^{k+q} t_{k-q} \quad [5]$$

As yet, no mention has been made of the coordinate systems used to describe the state of polarization. We will deal with primarily two different frames:

- (i) "Helicity" frame - in this frame, the z-axis is chosen individually for the description of each particle in the direction of its momentum in the centre of mass system. Each particle has a common y-axis perpendicular to the reaction plane in the direction  $\vec{p}_{in} \times \vec{p}_{out}$ , where  $\vec{p}_{in}$  and  $\vec{p}_{out}$  are the linear momenta of the incoming and outgoing particles, respectively.
- (ii) "Laboratory" frame - in this frame, all particles are described by the same set of axes with the z-axis chosen along the direction of the incident beam and the y-axis in the direction  $\vec{p}_{in} \times \vec{p}_{out}$ .

The helicity frame corresponds to the choice of the Madison convention, but in some circumstances the laboratory frame is preferable. There is another commonly used coordinate frame, the so-called "transversity" frame which will not be discussed here. Discussions of this are found in Simonius (1974).

Analyzing Powers - Cross Sections

Quantum mechanics tells us that the spin amplitudes of the final state may be expressed in terms of the spin amplitudes of the initial state by matrix elements of some transition operator,  $T$ , as

$$\begin{aligned}
 a_n^{out} &= \langle \chi_n^{out} | T | \psi^{in} \rangle \\
 &= \sum_{\mu} a_{\mu}^{in} \langle \chi_n^{out} | T | \chi_{\mu}^{in} \rangle \\
 &\equiv \sum_{\mu} a_{\mu}^{in} F_n^{\mu}
 \end{aligned}
 \tag{6}$$

Here we only show explicitly the dependence of the reaction amplitudes,  $F$ , on the spin variables. It follows that an element of the density matrix for the final state can be expressed in terms of density matrix elements for the initial state as

$$\rho_{mn}^{out} = \sum_{\mu\mu'} F_m^{\mu} \rho_{\mu\mu'}^{in} F_n^{*\mu'}
 \tag{7}$$

Using previous expressions for the tensor moments one finds that

$$t_{k'q'}^{out} = N \sum_{kq} T_{kq}^{k'q'} t_{kq}^{in}
 \tag{8}$$

with

$$\begin{aligned}
 T_{kq}^{k'q'} &= \frac{1}{N} \sum_{m\mu\mu'} (\gamma_{k'q'}^{s=J})_{m\mu} (\gamma_{kq}^{s=S_i})_{\mu\mu'} \\
 &\quad \times F_m^{\mu} F_n^{*\mu'}
 \end{aligned}
 \tag{9}$$

where  $N$  is a normalization constant, usually chosen such that  $T_{00}^{00} = 1$ . Here  $T_{kq}^{k'q'}$  is referred to as a polarization transfer coefficient and essentially expresses the dependence of the outgoing polarization on the incoming polarization. If it is desired only to measure the cross-



section with an incident polarized beam (i.e. we want to measure  $t_{00}^{\text{out}}$ ) then the appropriate expression is

$$\frac{d\sigma}{dn} = t_{00}^{\text{out}} = N \sum_{kq} T_{kq}^* t_{kq}^{\text{in}} \quad [10]$$

In this special case, the  $T_{kq} \equiv T_{kq}^{00}$  are referred to as analyzing powers and the normalization constant is simply the unpolarized cross-section. Since the cross-section is a scalar and hence invariant under rotations, the  $T_{kq}$  should have the same transformation properties as the  $t_{kq}$ . In particular, if the reaction conserves parity, then the symmetry about the reaction plane leads to

$$T_{kq} = (-1)^{k+q} T_{k-q} \quad [11]$$

in the helicity frame. Combining this relation with the analog of equation [4] gives

$$T_{kq}^* = (-1)^k T_{kq} \quad [12]$$

The expression for the cross-section can now be written more explicitly as (for spin 1 incident particles)

$$\frac{d\sigma}{dn} = \left( \frac{d\sigma}{dn} \right)_{\text{unpol}} \left\{ 1 + 2 \operatorname{Re}(it_{11}) i T_{11} + t_{20} T_{20} + 2 \operatorname{Re}(t_{22}) T_{22} + 2 \operatorname{Re}(t_{21}) T_{21} \right\} \quad [13]$$

It is useful often to express the reaction amplitudes in terms of a partial wave decomposition and thus separate out the angular dependence. For the helicity frame, this decomposition takes a particularly simple form (Jacob and Wick, 1959):

$$F_{\lambda'}^{\lambda} = \sum_J \frac{2J+1}{4\pi} f_{\lambda'}^{\lambda}(J) d_{\lambda\lambda'}^J(\theta) \quad [14]$$

The more complicated (but perhaps better known) expression for the partial wave decomposition in the laboratory frame is :

$$F_{m'}^m = \sum_{l_i, l_f, J} (l_i, 0, s_i, m | J, m) (l_f, m-m', J, m' | J, m) \\ \times f_{l_f}^{l_i}(J) \frac{(2l_i+1)(2l_f+1)}{4\pi} d_{m'-m, 0}^{l_f}(\theta) \quad [15]$$

Parity conservation in the reaction also leads to restrictions on the scattering amplitudes. For the helicity frame this takes the form of relationships between various amplitudes

$$F_{-\lambda'}^{-\lambda} = \pi_{tot} (-1)^{l_i + s_i + J} F_{\lambda'}^{\lambda} \quad [16]$$

where  $\pi_{tot}$  is the product of the intrinsic parities for the four particles involved in the reaction. In the laboratory frame, parity conservation leads to

$$f_{l_f}^{l_i}(J) = 0 \quad \text{if} \quad (-1)^{l_i + l_f} \neq \pi_{tot} \quad [17]$$

It is important to stress that the expressions above are model-independent and just represent a convenient way of dealing with angular momentum coupling and parity conservation. They represent a starting point for doing further calculations and provide the necessary interface between theory and experiment. All the nuclear physics information is contained in the reaction amplitudes,  $F$  (or  $f$  in the partial wave decomposition), which we have so far ignored. In order to calculate these, one must

assume some model of the reaction mechanism. In the next chapter the results will be presented for some calculations using the compound nucleus statistical model of nuclear reactions.

## CHAPTER II - The (d, $\alpha$ ) Reaction Near 0°

### Introduction

The formalism developed in the preceding chapter may be easily applied to the case of a (d, $\alpha$ ) reaction. If the deuterons are incident on an even-even target nucleus, then the spin structure for the reaction will be:

$$1^+ + 0^+ \rightarrow J^\pi + 0^+$$

where  $J^\pi$  labels the spin and parity of the state in the residual nucleus. If, in addition, the alpha particles are detected at 0° (or equivalently, 180°) to the beam direction then the expressions for the tensor analyzing power  $T_{20}$  assume particularly simple forms, and are model-independent for natural parity and  $J^\pi = 0^-$  states.

In this chapter, the expressions for  $T_{20}$  are first derived for the case where the alpha particles are detected on axis. Even at 0°, however, the expression for  $T_{20}$  for an unnatural parity state is model-dependent and therefore the probability of an unnatural parity state masquerading as a natural parity (or  $0^-$ ) state must be determined. This will be done later using the concept of Ericson fluctuations. Also the effect of detecting the alpha particles slightly off-axis will be investigated using the statistical theory of nuclear reactions.

### $T_{20}$ For Natural Parity and $0^-$ States

Recall that the analyzing powers are given in terms of the reaction

amplitudes as

$$T_{kq} = \frac{1}{N} \sum_{ijm} (\tau_{kq}^{s-1})_{ij} F_m^i F_m^{*j}$$

and that the reaction amplitudes can be further decomposed into an angle dependent part and an angle independent part:

$$F_m^i = \sum_J \frac{2J+1}{4\pi} f_m^i(J) d_{im}^J(\theta)$$

At  $\theta = 0^\circ$  the d-function gives  $F_m^i = 0$  unless  $i = m$ . This just expresses the conservation of angular momentum and means that, at  $0^\circ$ , all the analyzing powers are zero except  $T_{20}$  since  $(\tau_{kq})_{ii} \propto \delta_{q0}$ . Hence, using explicit expressions for the  $(\tau_{kq})$ , the cross-section for this reaction can be written simply as

$$\frac{d\sigma}{d\Omega} = \left( \frac{d\sigma}{d\Omega} \right)_{\text{unpol}} (1 + T_{20} t_{20}) \quad [1]$$

with

$$T_{20} = \frac{1}{\sqrt{2}} \frac{|F_{-1}^{-1}|^2 - 2|F_0^0|^2 + |F_1^1|^2}{|F_{-1}^{-1}|^2 + |F_0^0|^2 + |F_1^1|^2} \quad [2]$$

and

$$\left( \frac{d\sigma}{d\Omega} \right)_{\text{unpol}} = \frac{1}{3} \{ |F_{-1}^{-1}|^2 + |F_0^0|^2 + |F_1^1|^2 \} \quad [3]$$

The condition (Eq. 1.16) imposed on the scattering amplitudes by parity conservation in the reaction is

$$F_{-j}^{-i} = \pi (-1)^{i+j+l+J} F_j^i$$

For a natural parity state  $\pi = (-1)^J$  so that  $F_0^0 = 0$  and  $F_{-1}^{-1} = -F_1^1$  and

therefore the tensor analyzing power is

$$T_{20} = 1/\sqrt{2} \quad , \quad \pi = (-1)^J$$

independent of the reaction mechanism. A special case is that of a spin zero level, where the amplitudes  $F_{\pm 1}^{\pm 1}$  are not allowed. For  $J^\pi = 0^+$  we also have  $F_0^0 = 0$  and we get the well known result that

$$\left( \frac{d\sigma}{d\Omega} \right)_{\text{unpol}} = 0 \quad , \quad J^\pi = 0^+$$

For a  $J^\pi = 0^-$  state on the other hand,

$$T_{20} = -\sqrt{2} \quad , \quad J^\pi = 0^-$$

Natural parity states and  $0^-$  states represent the possible limits for  $T_{20}$ . In general, a state of unnatural parity can have values of  $T_{20}$  anywhere between the two limits including the limits themselves, depending on the ratio  $F_0^0/F_1^1$ , and will therefore be model-dependent. It is again important to emphasize that these results are model-independent and rely on only the conservation laws of angular momentum and parity. In fact, this reaction at  $0^\circ$  can be a useful method for determining the tensor polarization of a spin-1 beam.

#### Unnatural Parity States - Ericson Fluctuations

In practice, if  $T_{20}$  is measured for a state of unknown spin or parity, and it is found to be within but not on the limits, then an unambiguous assignment of unnatural parity can be made. If, however it is found to be at either limit within error, then an assignment of natural parity or  $0^-$  can only be made if  $T_{20}$  remains at the limit for several other energies. With this in mind, it is of some interest to determine what can be expected

in terms of the distribution of tensor analyzing powers for an unnatural parity state. In other words, what is the probability that a state with  $T_{20} = -\sqrt{2}$  or  $1/\sqrt{2}$  (within experimental error) has unnatural parity?

In the usual statistical model of nuclear reactions (Brink and Stephen, 1963; Ericson, 1963) the scattering amplitudes  $F$  (the indices will be suppressed for the time being) are written as the sum of an average part  $f_0$  and a fluctuating part  $f_c$

$$F(E) = f_0 + f_c$$

where the fluctuating part can be represented as a superposition of resonance terms. The amplitudes of each resonance term are assumed real or complex random variables and if we are in a region of overlapping levels  $f_c$  will have an approximately normal probability distribution with a mean of zero. The average (over energy) of the square of the amplitudes will then be

$$\begin{aligned} \langle F^2 \rangle &= \langle (f_0 + f_c)(f_0^* + f_c^*) \rangle \\ &= |f_0|^2 + \langle f_c f_c^* \rangle \end{aligned}$$

This defines the "direct" contribution  $|f_0|^2$  which comes from the average part and the "compound nucleus" contribution which comes from the fluctuating part.

Now let us consider the case where the average part of the scattering amplitudes are zero, i.e. a pure compound nuclear reaction. This case will likely give rise to the largest fluctuation of the tensor analyzing power and hence will represent the "worst" case. Here it is clear that  $|F|^2$  will have, by

definition a  $\chi^2$  distribution with two degrees of freedom, viz

$$P(x) \propto \exp(-x/\langle x \rangle)$$

where  $x$  represents  $|F|^2$  and  $\langle x \rangle$  its mean value (over energy). If we have a thick target or average measurements taken at several beam energies then the probability distribution becomes

$$P(x) \propto \left(\frac{x}{\langle x \rangle}\right)^{N-1} \exp(-x/\langle x \rangle) \quad [4]$$

where  $N$  is related to the target thickness and corresponds roughly to the energy loss of the beam in the target in units of the coherence width. This same distribution of amplitudes would be obtained if one carried out an energy average over  $N$  different energies separated by at least the coherence width. Indeed, since this method is expected to have its widest range of applicability in light nuclei, targets thick enough to correspond to  $N \gg 1$  will, in general, be impractical to use because of resolution effects and therefore an average of the cross-sections for a number of energies will have to be made.  $\square$

It is fairly straightforward to show that the distribution of  $T_{20}$  in equation [2] resulting from the distribution of amplitudes of equation [4] is given by

$$P(T_{20}) \propto \frac{\{(T_{20} + \sqrt{Z})(\sqrt{Z} - 2T_{20})\}^{N-1}}{\{\langle |F_1|^2 \rangle (\sqrt{Z} - 2T_{20}) + \langle |F_0|^2 \rangle (T_{20} + \sqrt{Z})\}^{2N}} \quad [5]$$

This equation involves the average values for the amplitudes  $\langle |F|^2 \rangle$  and hence we must obtain some estimate for them. Using a statistical weight argument, valid for many  $l$ -values contributing in the reaction, Boerma



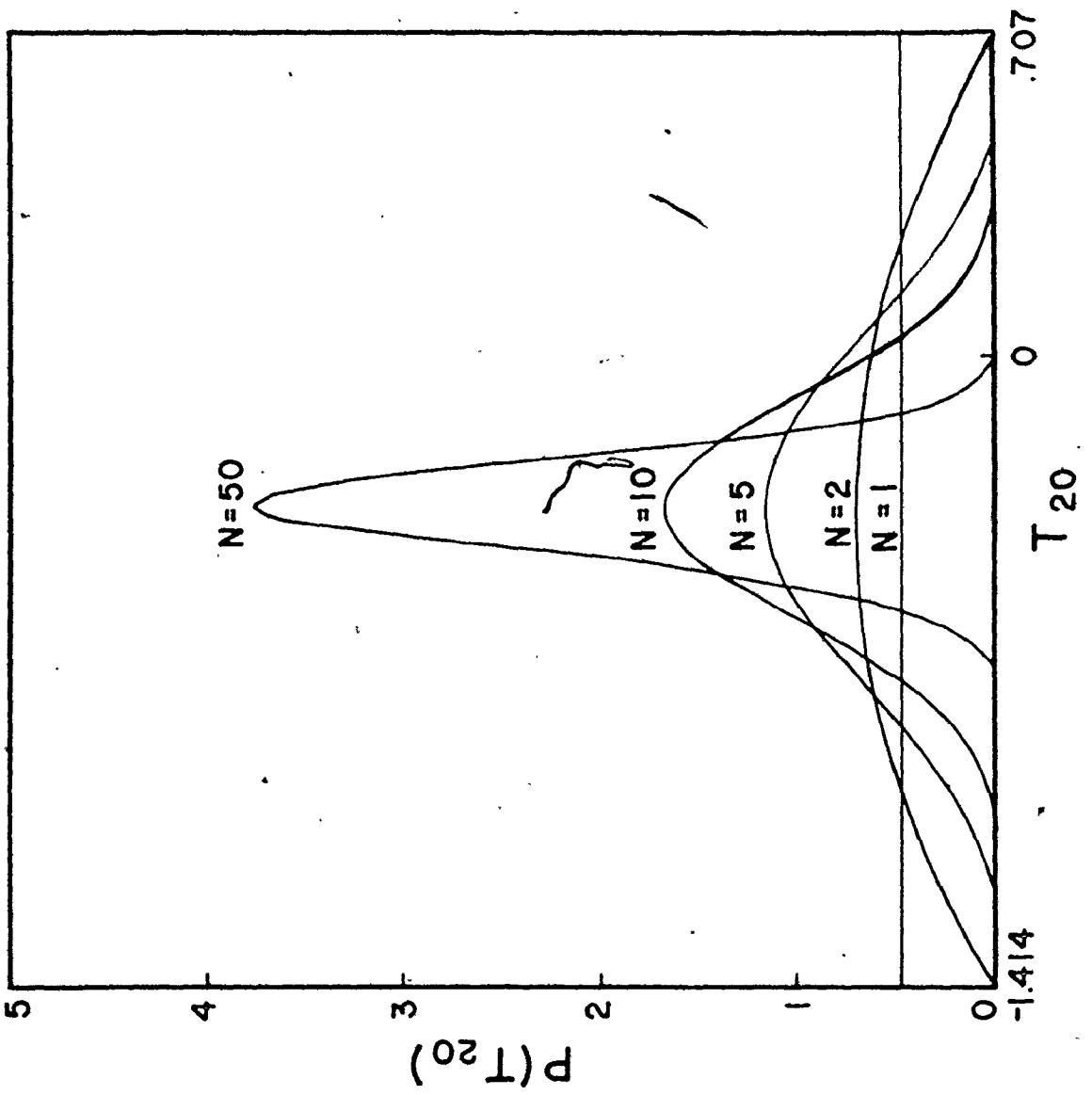
et.al. (1975), have shown that the mean values of the amplitudes in the compound nuclear model are related by

$$\langle |F_0^0|^2 \rangle = 2 \langle |F_1^1|^2 \rangle \quad [6]$$

For the case of a thin target and a single energy, where  $N = 1$ , equation [5] then becomes  $P(T_{20}) = \text{constant}$ . For an energy average, on the other hand, the distribution will no longer be uniform and will have a maximum value at  $T_{20} = -1/(2\sqrt{2})$ . In Fig. 2.1, the distribution [5] is shown plotted for values of  $N = 1, 2, 5, 10$ , and 50. It should be noted that the assumption [6] for the mean values is only approximately correct and for low beam energies the peak in the distribution will shift towards  $T_{20} = 0$ . Figure 2.2 shows the distribution with  $N = 3$  for various ratios of  $\langle |F_0^0|^2 \rangle / \langle |F_1^1|^2 \rangle$ . Using equation [5] one can estimate the reliability of assignments of natural parity or  $0^-$  to a state. Obviously, the larger the number of measurements the more confidence one would have in making an assignment. To be more quantitative Table 2.1 shows the values of the cumulative probability for deviations of 0.05, 0.1, 0.2, and 0.4 from the limits of  $T_{20}$  ( $-1/\sqrt{2}$  or  $1/\sqrt{2}$ ). For example, the table shows that for  $N = 3$  the probability of obtaining an average value of  $T_{20}$  for an unnatural parity state closer than 0.1 to either limit is 0.1%. It is clear that  $N \geq 3$  will usually suffice to be confident of an assignment of natural parity or  $0^-$  to a level. If direct processes contribute significantly to the reaction, then fluctuations will be damped and the probability of an unnatural parity state having a value of  $T_{20}$  near either limit will be reduced.

Figure 2.1

Probability distribution of the tensor analyzing power,  $T_{20}$ , for unnatural parity states in the  $(\vec{d}, \alpha)$  reaction corresponding to different values of  $N$ .  $N$  refers to the thickness of the target in units of the coherence width or, alternatively, to the number of different energies for which the data are averaged.



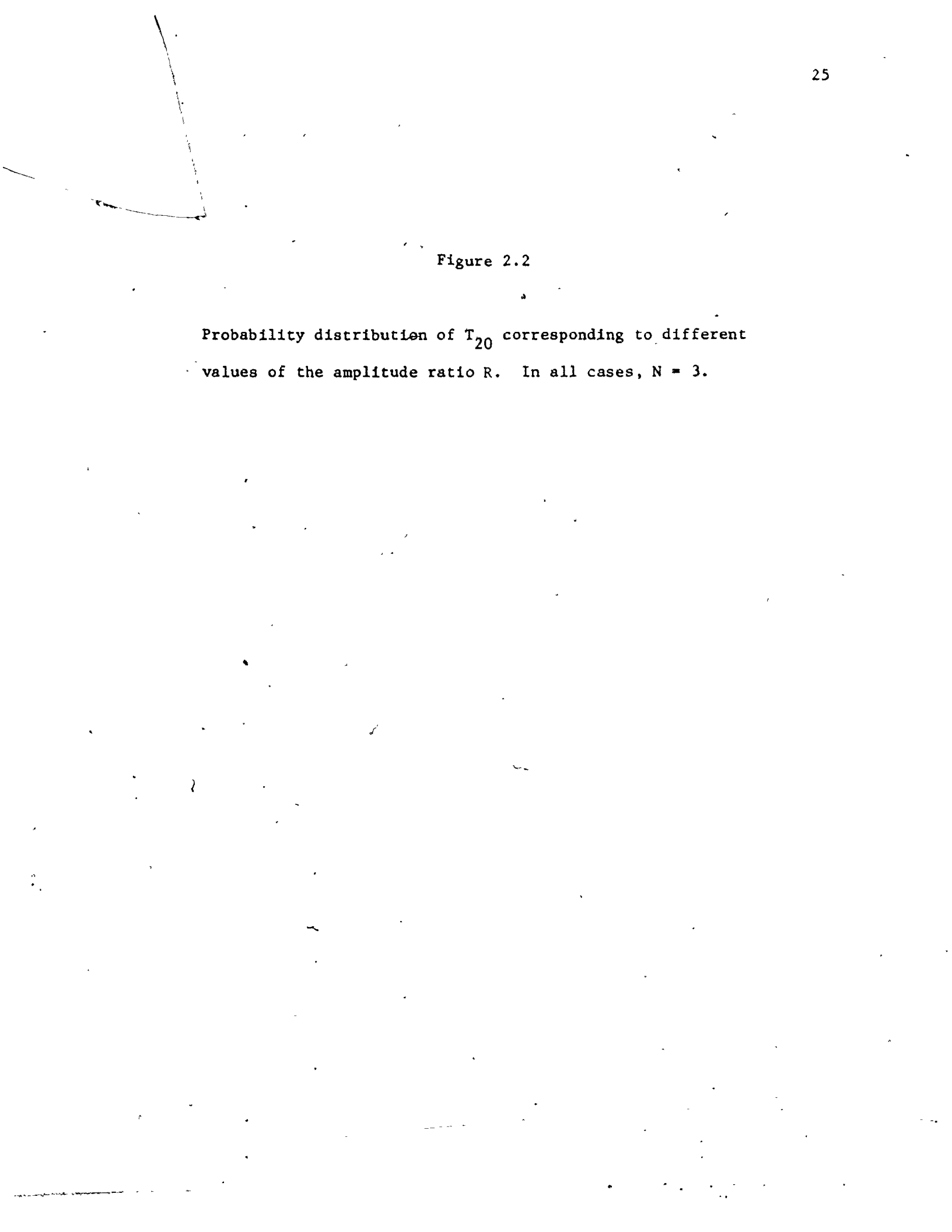


Figure 2.2

Probability distribution of  $T_{20}$  corresponding to different values of the amplitude ratio  $R$ . In all cases,  $N = 3$ .

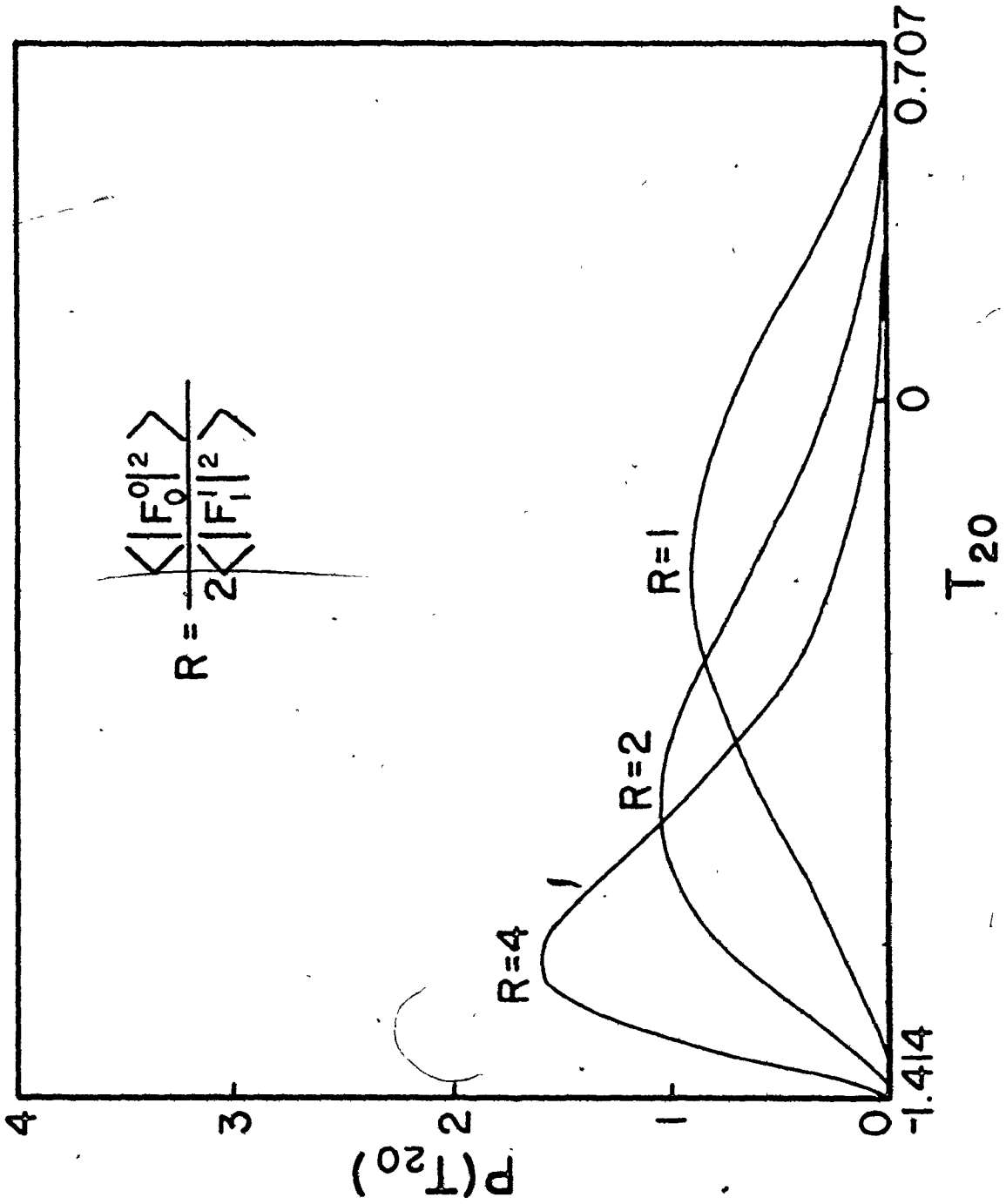


Table 2.1

Values of the cumulative probability for various deviations,  $\Delta$ , from the limits of  $T_{20}$  ( $-\sqrt{2}$  or  $1/\sqrt{2}$ )

Number of Energies N	Cumulative Probability <sup>a)</sup>			
	$\Delta=.05$	$\Delta=0.1$	$\Delta=0.2$	$\Delta=0.4$
1	2.5%	4.5%	9.5%	19%
2	.1%	.7%	2.7%	9.5%
3		.1%	.8%	5.4%
4			.2%	3.0%
5			.1%	1.6%
10				.1%

a) Values not shown are less than 0.1%

### Deviations From $0^\circ$ - Compound Statistical Model

One effect not yet discussed is that of detecting the alpha particles slightly off-axis. In this case the expression for the tensor analyzing power for natural parity or  $0^-$  states becomes more complicated than equation [2] and is no longer model-independent. In order to estimate the average attenuation of  $T_{20}$  that one could expect, a statistical model calculation was performed.

The statistical model for nuclear reactions (Hauser and Feshbach, 1952; Feshbach, 1960; Ericson, 1960) is based on the premise that the reaction proceeds through a large number of overlapping states in the compound nucleus. This model is approximately valid for the reactions and energies studied here (Jänecke, 1963). In this case interference terms between different channels average to zero and the general form for the (energy - averaged) reaction amplitudes can be written in terms of incident and exit transmission coefficients. The transmission coefficients will, in general, be functions of the incident and exit orbital angular momenta, and to a first approximation can be represented by Coulomb penetrabilities. In the laboratory frame the partial wave scattering amplitudes of equation 1.15 will then be

$$f_{l_f}^{l_i} (J) f_{l_f'}^{l_i'} (J) \propto \delta_{l_i l_i'} \delta_{l_f l_f'} T_{l_i} T_{l_f}$$

The Coulomb penetrabilities were computed using standard techniques (Blatt and Weisskopf, 1952; Fröberg, 1955) and for these calculations provided a natural cutoff at around  $l = 10$ . Since the results will depend on only the beam energy, the energy of the final state and the target nucleus radius, calculations were carried out for incident deuteron beam

energies of 5, 10, 15 MeV on targets of  $^{12}\text{C}$ ,  $^{24}\text{Mg}$ , and  $^{40}\text{Ca}$  and corresponding to an excitation energy in the residual nucleus of about 2 MeV. It was felt that these would provide information over a wide range of experimental conditions and the results for any cases not covered could be interpolated from them. Some sample angular distributions for the tensor analyzing power of a natural parity state are shown in Figure 2.3 and the next chapter presents some data for a particular case. The attenuation at  $2^\circ$  (the angle used in this experiment and at  $5^\circ$  (which corresponds roughly to using an annular counter at  $180^\circ$ ) of the value of  $T_{20}$  expected for a natural parity or  $0^-$  state is shown in Table 2.2. It is apparent that  $2^\circ$  is close enough to  $0^\circ$  to be useful but in some circumstances  $5^\circ$  may not be.



Figure 2.3

Calculated angular distribution near  $0^\circ$  for the tensor analyzing power of a natural parity state. The dashed line refers to the reaction  $^{12}\text{C}(d,\alpha)^{10}\text{B}$  at  $E_d = 5$  MeV and the solid line refers to the reaction  $^{40}\text{Ca}(d,\alpha)^{10}\text{B}$  at  $E_d = 15$  MeV. Both calculations are for a state about 2 MeV in excitation in the final nucleus and having  $J^\pi = 1^-$ , although the results are quite insensitive to the spin of the final state.

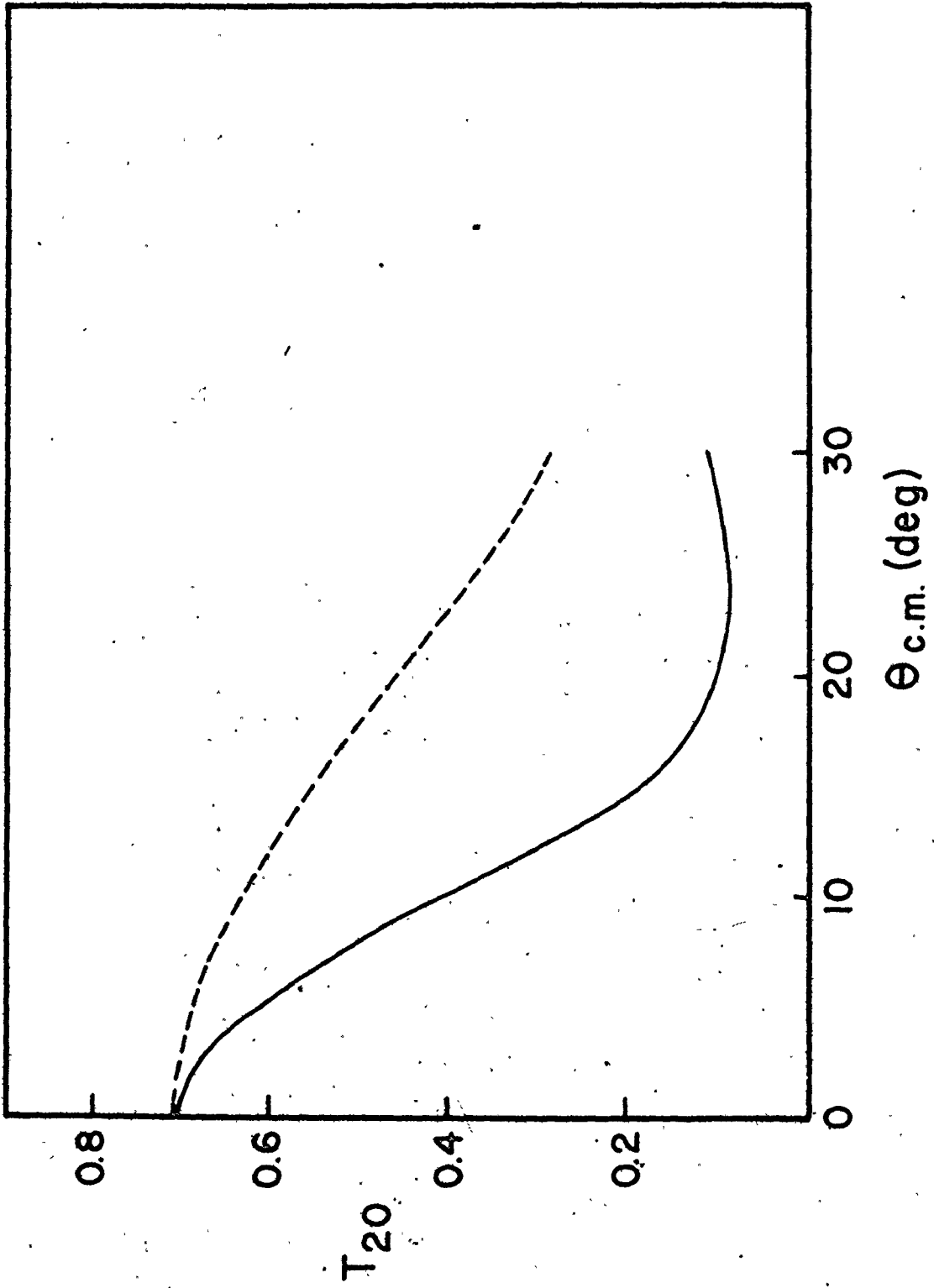


Table 2.2

Calculated attenuation of  $T_{20}$  for natural parity states  
when detecting alpha particles slightly off-axis

Target	Incident Energy (MeV)	Attenuation (%)	
		$\theta_{cm} = 2^\circ$	$\theta_{cm} = 5^\circ$
$^{12}\text{C}$	5	0.4	2.5
$^{12}\text{C}$	10	0.7	5.2
$^{12}\text{C}$	15	1.3	7.6
$^{24}\text{Mg}$	5	0.3	2.0
$^{24}\text{Mg}$	10	0.7	5.0
$^{24}\text{Mg}$	15	1.3	8.0
$^{40}\text{Ca}$	5	0.4	3.1
$^{40}\text{Ca}$	10	1.1	7.6
$^{40}\text{Ca}$	15	2.1	12.0

## CHAPTER III - The $^{12}\text{C}(d,\alpha)^{10}\text{B}$ and $^{16}\text{O}(d,\alpha)^{14}\text{N}$ Experiments

### Introduction

Since the cross-section for the (d, $\alpha$ ) reaction is several times larger for  $^{12}\text{C}$  and  $^{16}\text{O}$  targets than it is for heavier mass nuclei such as  $^{24}\text{Mg}$  and  $^{40}\text{Ca}$ , and since the level spacings in the final nuclei are fairly large, it was decided to use these reactions as a test of the method of parity determination. In addition to proving the feasibility of the method these experiments were able to provide new information for  $^{10}\text{B}$  and  $^{14}\text{N}$  and confirm some previously model-dependent assignments (Kuehner et al., 1975; Petty et al. 1976a).

The final experimental configuration, which will be described in the next section, was the result of many different (and mostly unsuccessful) attempts over a period of about 18 months. The detection of alpha particles with an annular counter at  $180^\circ$  suffers from two main disadvantages:

- (i) The resolution that one can obtain in practice ( $\approx 50$  keV) is often not sufficient to resolve the peaks of interest; and,
- (ii) As pointed out in the previous chapter, the attenuation of  $T_{20}$  expected for natural parity and  $0^-$  states may, in some cases, lead to incorrect assignments of unnatural parity.

These disadvantages are partially offset however by the much greater solid angle subtended by the detector and hence, the shorter running times that are required. This technique of detection near  $180^\circ$  has been used by at least two groups to date (Boerma et al., 1975; Rickel et al., 1976). The detection of alpha particles near  $0^\circ$  has the major disadvantage

that there is a very large flux of longer-range deuterons present which must in some way be discriminated against. It was found that it was not possible to run at  $0^\circ$ , but at  $2^\circ$  ( $3^\circ$  in the case of the  $^{40}\text{Ca}$  experiments) the background flux was sufficiently reduced to allow measurements to be made.

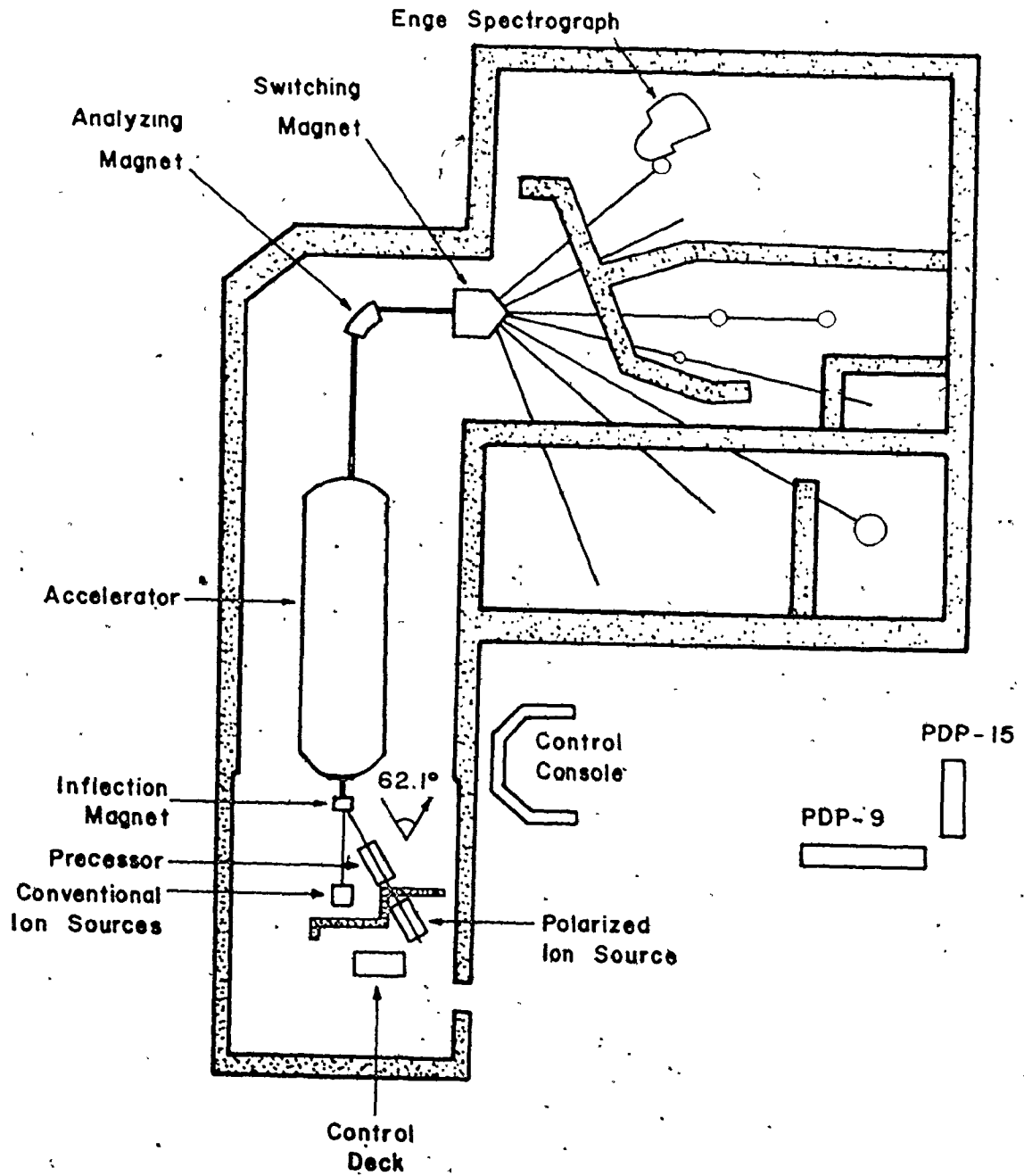
### Experimental Details

The general accelerator layout is shown in Figure 3.1. A polarized deuteron beam was produced by the recently installed McMaster Lamb-shift polarized ion source and accelerated through an FN tandem accelerator. Alpha particles from the reaction were momentum analyzed with an Enge split-pole magnetic spectrograph and detected on the focal plane with a position-sensitive gas proportional counter. These various aspects will be discussed below.

The theory and operation of the polarized ion source have been described in detail elsewhere (Ohlsen, 1970; McKay, 1976) and only the salient features will be mentioned here. This source can produce negative deuterium ions with the nucleus having variable amounts of vector and/or tensor polarizations. In the configuration used in these experiments (i.e. a high argon magnetic field) the deuterons can be considered to be in a particular magnetic substate, where the quantization axis is parallel to the beam direction. In addition there is always a certain amount of deuterons present which are essentially unpolarized. The ratio of the total beam current to that portion which is unpolarized is defined as the quench ratio  $Q$ . The fractional beam polarization  $P$  represents the ratio of the polarized beam component to the total beam current and is related simply to the quench ratio as  $P = 1 - 1/Q$ . Usual operation of the ion source will

Figure 3.1

General layout for the FN tandem accelerator and associated beam lines at McMaster University.



produce beams with P from 60 to 80 %. Table 3.1 shows the values of  $t_{20}$  and  $t_{10}$  as a function of the magnetic substate of the beam and represents the polarization of the beam as it emerges from the source. Since the spin quantization axis does not rotate as fast as the deuteron momentum vector in the fields of the inflection, analyzing and switching magnets, it is necessary to provide an additional rotation of the quantization axis. This is accomplished by a set of crossed electric and magnetic fields (Wien filter) at the exit from the source and is labelled as the spin precessor in Figure 3.1. The angle of  $62.1^\circ$  shown in the figure represents the amount of rotation needed for a deuteron beam so that the quantization axis will be aligned along the beam direction when the beam enters the target chamber of the Enge spectrograph.

The target chamber is shown schematically in Figure 3.2. There are no slits in the system after the switching magnet since it was found that small-angle scattering of the beam from any set of slits present resulted in an excessive background in the detector. Focussing and steering of the beam was realized with two quartz viewers before the chamber and a 1 mm dia. aperture that could be placed in the target location. The Faraday cup rotated with the spectrograph and allowed angular distributions to be measured to  $30^\circ$ .

A schematic of the proportional counter is shown in Figure 3.3. It has an active length of 30 cm. and is of the resistive wire type (Fulbright et.al., 1973) using a gas mixture of 90% argon and 10% methane. Particles enter the chamber through a thin aluminized mylar window and produce electron-ion pairs along their path. Amplification takes place near the anode wire with the result that a net charge builds up on the wire. This charge



Table 3.1

Vector and tensor polarization as a function of the magnetic substate of the beam and the fractional beam polarization

	$m = +1$	$m = 0$	$m = -1$
$t_{10}$	$\frac{\sqrt{3}}{2} P$	0	$-\frac{\sqrt{3}}{2} P$
$t_{20}$	$\frac{P}{\sqrt{2}}$	$-\sqrt{2} P$	$\frac{P}{\sqrt{2}}$

where:

$P =$  Fractional beam polarization  $= 1 - 1/Q$

$Q =$  Quench ratio

Figure 3.2

Schematic of the target chamber setup on the Enge spectrograph. The Faraday cup is made of tantalum and is attached to the entrance tube of the magnet by a Teflon insert. The target holder also holds a 1mm dia. tantalum aperture which can be placed in the target position.

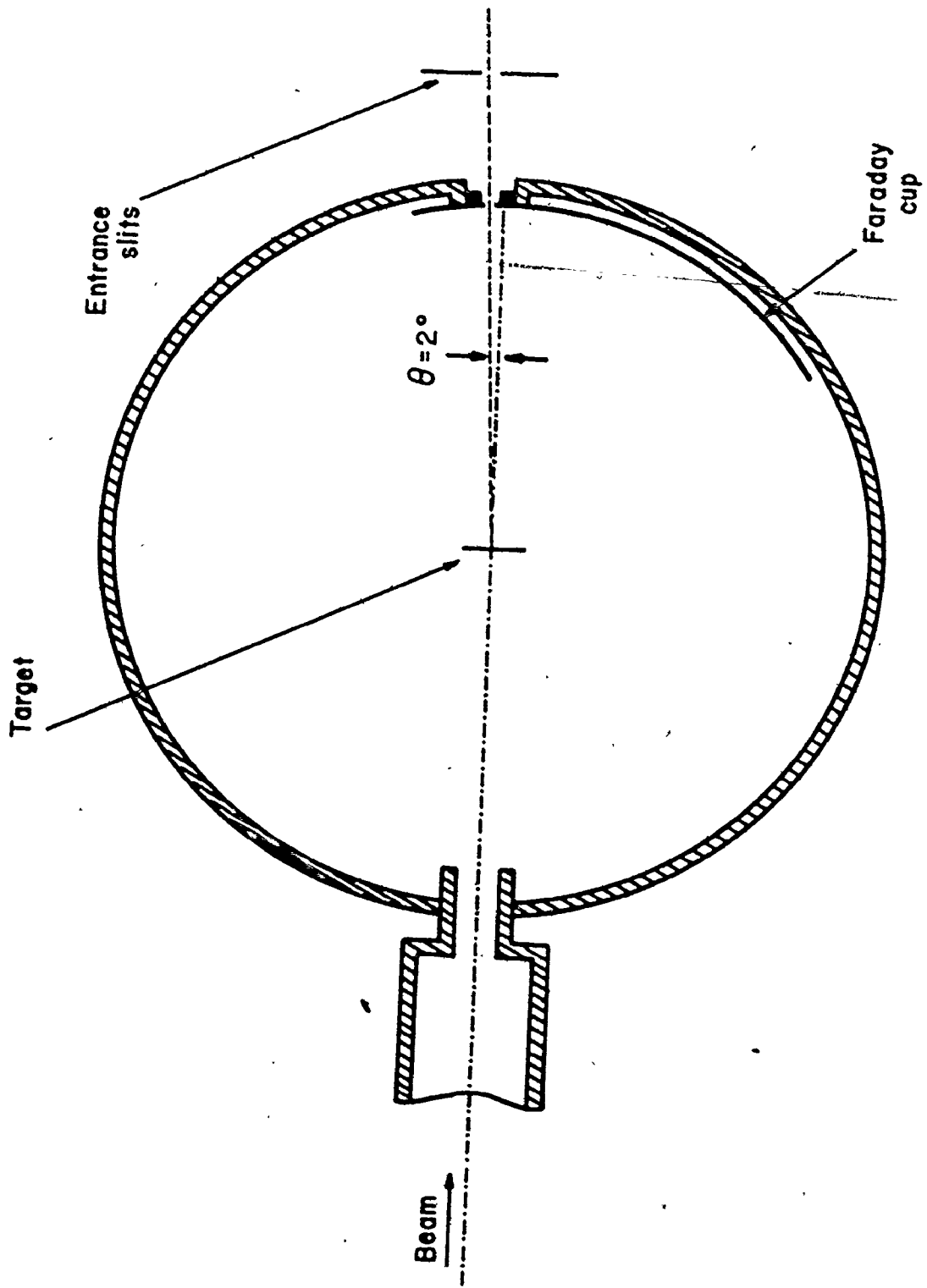
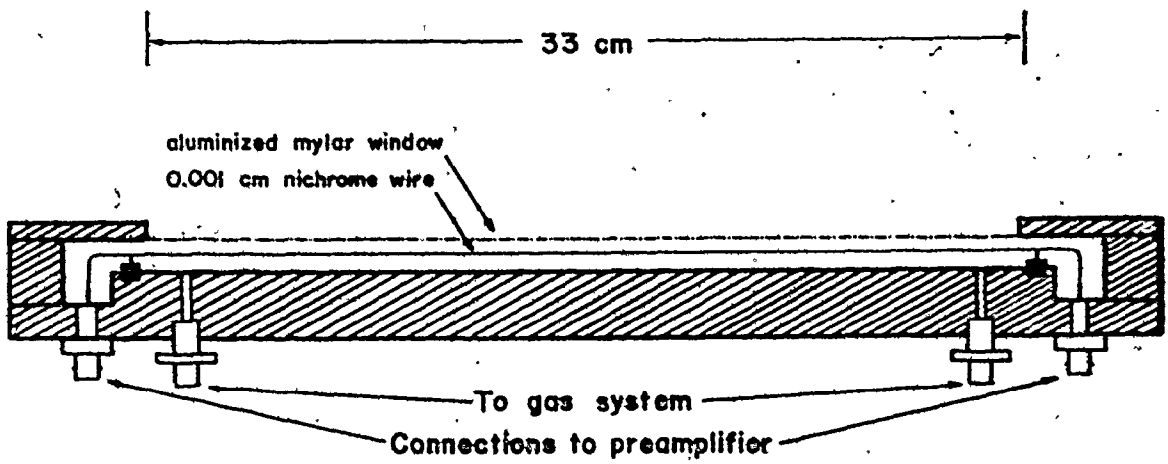


Figure 3.3

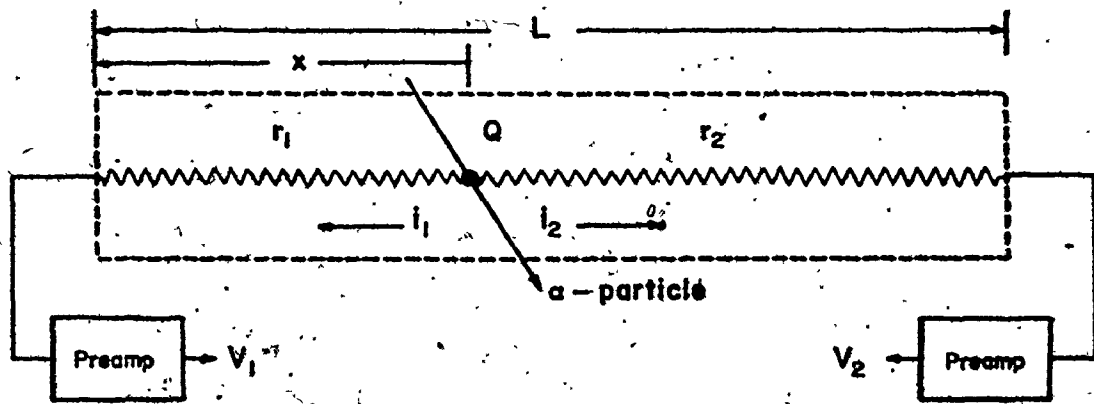
Position-sensitive proportional counter schematic drawings.

Part (a) shows the physical construction of the device. The nichrome wire is indium-soldered to terminals at either end which are in turn connected to the signal feedthroughs. This permits separate replacement of either the wire or the feedthroughs. Part (b) schematically outlines the physical operation of the counter.

(a)



(b)



$$\frac{V_2}{V_1 + V_2} = \frac{x}{L}$$

then divides and flows to either end with the relative sizes of the currents inversely proportional to the distance from the ends. After appropriate amplification these pulses are then sent to the computer where the information is used to update spectra in memory. The total signal produced gives information on the energy deposited by the particle in the counter thus allowing particle identification. This allows us to discriminate against the large background flux of deuterons present. The intrinsic position resolution of this detector is about 1mm and further details can be found in the users' guide (Petty, 1974).

The electronics setup is very simple and is shown schematically in Figure 3.4. In order to compensate for the dead time in the counter and in the on-line computer, the beam was pulsed off for about 200  $\mu$ sec after each event was detected.

#### The $^{12}\text{C}(d,\alpha)^{10}\text{B}$ Reaction

Alpha particle spectra were taken at lab angles of  $2^\circ$ ,  $5^\circ$ ,  $10^\circ$ , and  $20^\circ$  for beam energies of 13.6 and 14.5 MeV. The target used was an  $80 \mu\text{g}/\text{cm}^2$  natural C foil. Runs were taken for  $m = 0$  and unpolarized deuterons and with an average beam current of 30 nA they lasted about 10 minutes. Because of the large energy dispersion of the spectrograph, only a portion of the spectrum of  $^{10}\text{B}$  could be recorded in one run and different bites were taken corresponding to excitation energies in  $^{10}\text{B}$  of roughly 0 to 2.15, 3.59 to 5.18, and 5.92 to 6.56 MeV. Figure 3.5 shows the spectra obtained for  $m = 0$  and unpolarized beam at 14.5 MeV. The ratio of the cross-sections for  $m = 0$  and unpolarized is plotted in part (c) of the figure. Table 3.2 lists the relationships between the cross-section ratio, fractional beam polarization, and tensor analyzing power appropriate to these experiments.

Figure 3.4

Electronics setup for the experiments. The beam was pulsed off by applying a 600 volt potential difference across the low energy x-steerers on the accelerator.

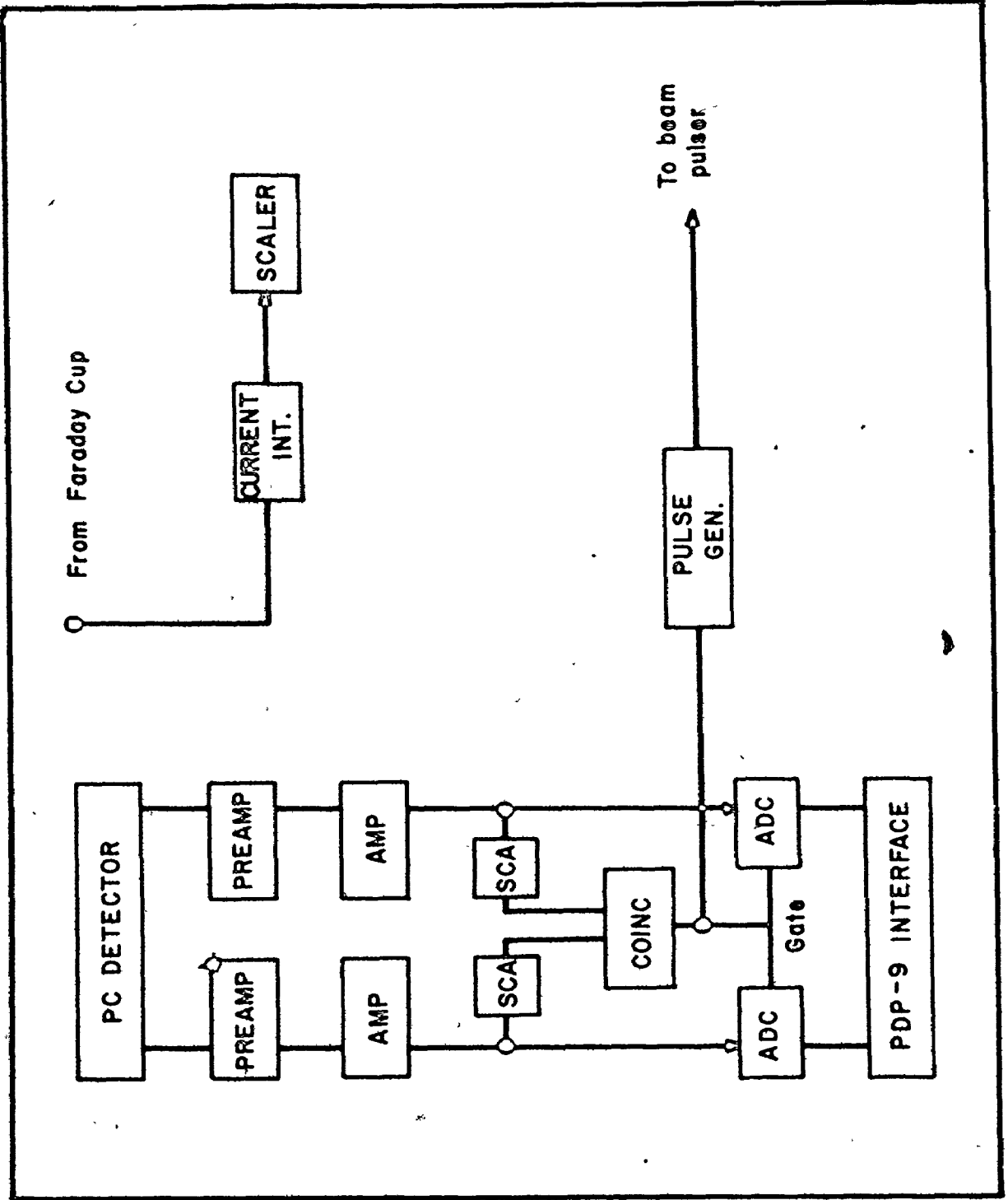




Figure 3.5

Spectra for the  $^{12}\text{C}(d,\alpha)^{10}\text{B}$  reaction at  $E_d = 14.5$  MeV and  $\theta_{\text{lab}} = 2^\circ$ . The upper spectrum (a) is taken for an unpolarized deuteron beam and the middle spectrum (b) is taken for the deuteron beam polarized in its  $m = 0$  substate. In (c) the ratio of the yield for the polarized beam to that for an unpolarized beam is plotted for each level. States of natural parity are expected to have a ratio of 0.28, the dashed line in the figure.

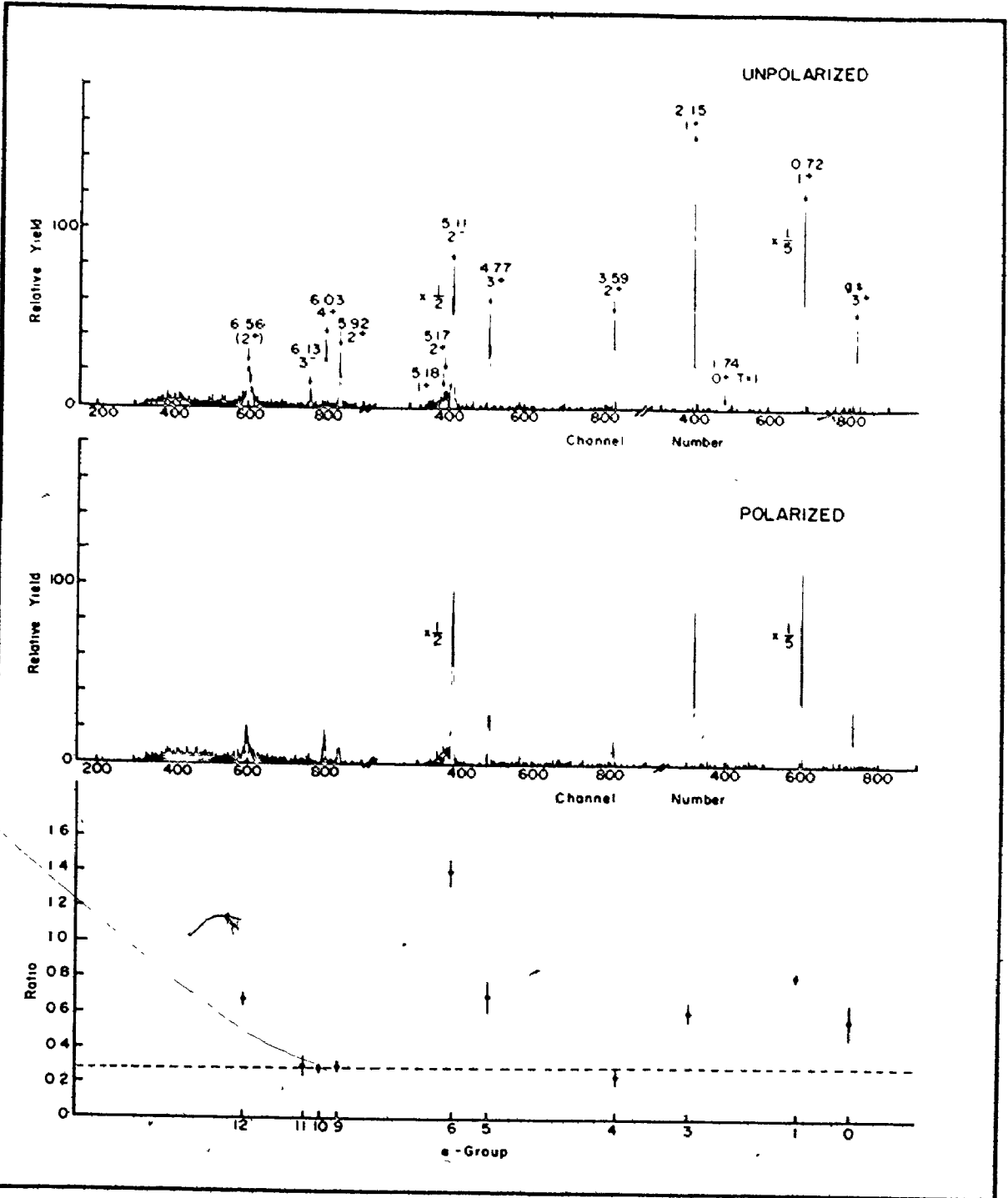


Table 3.2

Relationships between tensor analyzing power, fractional beam polarization, and yield ratios at  $0^\circ$

(a) Calculation of  $T_{20}$  from R.

$$R = \sigma(m=0)/\sigma(m=1)$$

$$R = \sigma(m=0)/\sigma(\text{unpol})$$

$T_{20}$

$$\frac{1}{\sqrt{2}P} \left( \frac{1-R}{1+R/2} \right)$$

$$\frac{1}{\sqrt{2}P} (1-R)$$

(b) Calculation of P from yield ratios for natural parity or  $0^-$  states.

$$R = \sigma(m=0)/\sigma(m=1)$$

$$R = \sigma(m=0)/\sigma(\text{unpol})$$

natural  
parity

$$\frac{1-R}{1+R/2}$$

$$1-R$$

$0^-$

$$\frac{R-1}{R+2}$$

$$\frac{R-1}{2}$$

where:

P = Fractional beam polarization

R = Yield ratio

$T_{20}$  = Tensor analyzing power

The results are consistent with the spin and parity assignments listed in the compilation (Ajzenberg-Selove and Lauritsen, 1974) with the exception of the 6.56 MeV level which is listed as  $2^+$ . An R-matrix analysis of the reaction  ${}^9\text{Be}(p,d){}^8\text{Be}$  (Sierk and Tombrello, 1973) appears to require  $2^+$  or  $3^+$ , consistent with  ${}^9\text{Be}({}^3\text{He},d){}^{10}\text{B}$  stripping data (Forsyth et. al., 1966), although an analysis of  ${}^6\text{Li}(\alpha,\alpha){}^6\text{Li}$  seems to favor  $\ell = 3$  and hence odd parity (Meyer et. al., 1967). If one disregards the scattering result as suggested by Sierk and Tombrello, then the present measurement would allow an unique  $3^+$  assignment.

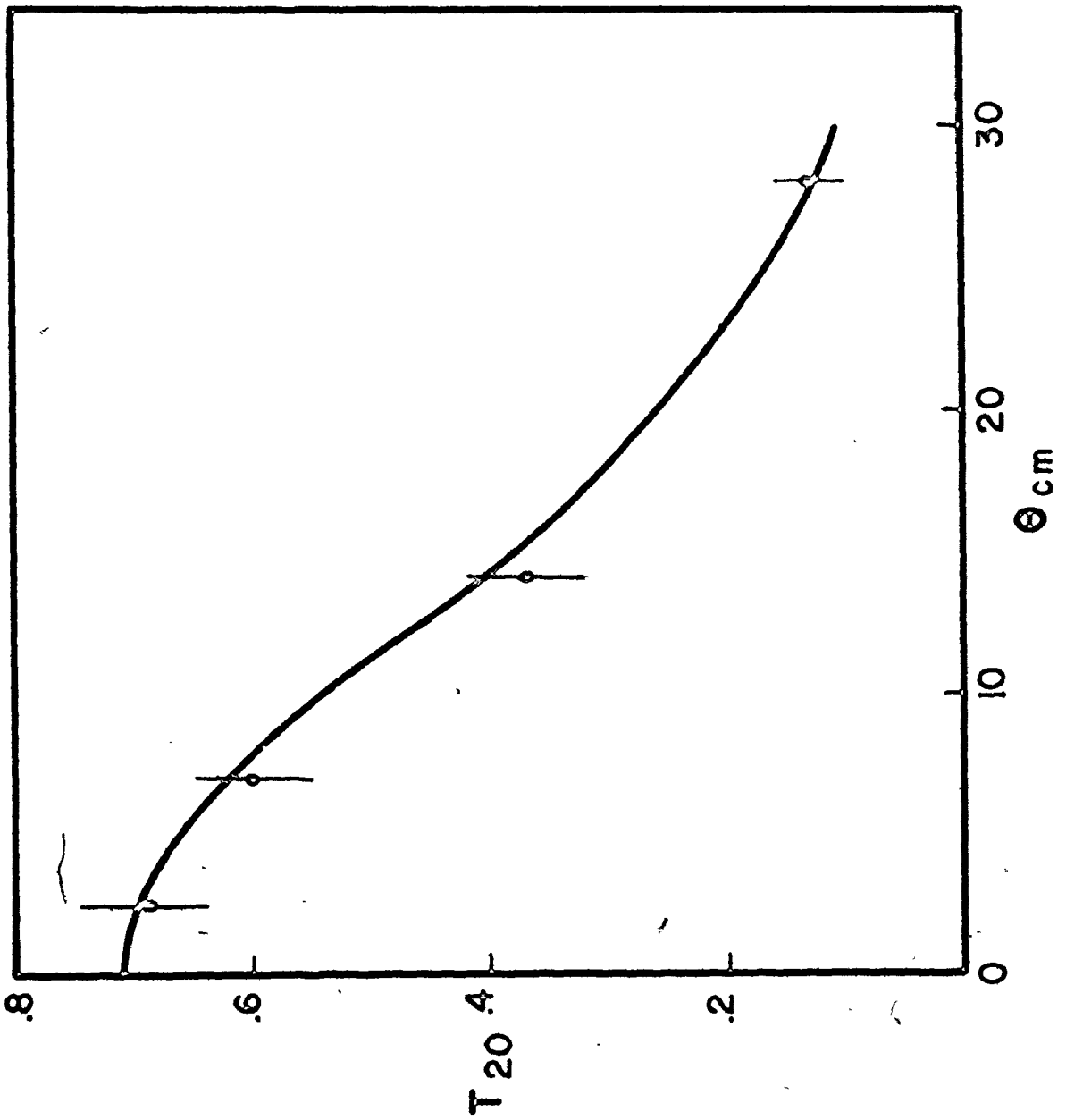
Figure 3.6 shows an angular distribution of the tensor analyzing power for the 3.59 MeV ( $2^+$ ) level calculated by averaging the data taken at 13.6 and 14.5 MeV. The solid line is Hauser-Feshbach calculation for this case, similar to those shown in the previous chapter. The fractional beam polarization was calculated by first obtaining an estimate from the ratio of the natural parity states. This value would tend to underestimate the polarization slightly. The  $2^\circ$  and  $5^\circ$  points were then fitted to a parabola with  $T_{20}(0^\circ) = 1/\sqrt{2}$ , since  $T_{20}$  is expected to go as  $\theta^2$  for small  $\theta$  (this comes from expanding the d-functions in the expressions for the scattering amplitudes). Agreement here is somewhat better than expected but it is clear that  $2^\circ$  will be close enough to  $0^\circ$  to be useful.

#### The ${}^{16}\text{O}(d,\alpha){}^{14}\text{N}$ Reaction

Alpha particle spectra were taken at  $2^\circ$  at beam energies of 11, 12, 13, and 14 MeV. The target used was an  $80 \mu\text{g}/\text{cm}^2$   $\text{GeO}_2$  layer evaporated onto a  $10 \mu\text{g}/\text{cm}^2$  C backing. The solid angle subtended by the entrance slits to the spectrograph was 0.9 msr and the angular range was  $1.2^\circ - 2.8^\circ$ . Runs were taken corresponding to excitation energies in  ${}^{14}\text{N}$  of roughly 4.91

Figure 3.6

Calculated and experimental angular distributions near  $0^\circ$  for the tensor analyzing power of the  $^{12}\text{C}(d,\alpha)^{10}\text{B}$  ( $2^+$ , 3.59 MeV) reaction. The solid line corresponds to a Hauser-Feshbach calculation at  $E_d = 14$  MeV and the points are data averaged for the energies  $E_d = 13.6$  and 14.5 MeV.



to 7.03 MeV and 7.97 to 9.13 MeV. At the same time the  $^{12}\text{C}$  backing provided alpha spectra of  $^{10}\text{B}$  corresponding to excitation energies from 0 to 4.77 MeV. For each beam energy and bite of the spectrum, runs were taken for deuterons polarized first in the  $m = 0$  substate and second for the  $m = 1$  substate. Each run lasted roughly two hours with an average beam current of 20 nA and all runs were normalized to the same total integrated current. The fractional beam polarization was determined by measuring the cross section ratio for known natural parity states in  $^{10}\text{B}$  and  $^{14}\text{N}$ . It was found to be constant within 5% during a three day period with an average value of 65%.

The spectra taken at 12 MeV are plotted in Figure 3.7. States in  $^{14}\text{N}$  are labelled with their excitation energies and those arising from the  $^{12}\text{C}$  backing are shown and labelled with the excitation energies. Excitation energies for  $^{10}\text{B}$  are taken from Ajzenberg-Selove and Lauritsen (1974) while those for  $^{14}\text{N}$  are taken from Ajzenberg-Selove (1976). Tensor analyzing powers at  $2^\circ$  for states in  $^{14}\text{N}$  from 4.91 to 9.13 are shown plotted in Figure 3.8. Tensor analyzing powers were also determined for states in  $^{10}\text{B}$  from 0 to 4.77 MeV and are shown in Figure 3.9. States with known natural parity have  $T_{20}$  of  $1/\sqrt{2}$ . In the figures,  $T_{20}$  is plotted from left to right for beam energies from 11 to 14 MeV, with the exception of the 6.20 and 7.03 MeV levels for which data are only available for three energies. The errors shown are based only on the statistical uncertainty in the peak areas and on the uncertainty in the beam polarization. It should be pointed out that the probability distributions derived in the previous chapter apply only when the cross-sections for  $m = 0$  and  $m = 1$  are averaged before  $T_{20}$  is calculated, and not for an average of  $T_{20}$  calculated at each energy. How-

Figure 3.7

Spectra for the  $^{16}\text{O}(\vec{d},\alpha)^{14}\text{N}$  reaction at  $E_d = 12$  Mev and  $\theta_{\text{lab}} = 2^\circ$ . The upper spectra are taken for the incident deuteron beam polarized in its  $m = 0$  substate and the lower spectra for the  $m = 1$  substate, where the quantization axis is aligned along the incident beam direction.



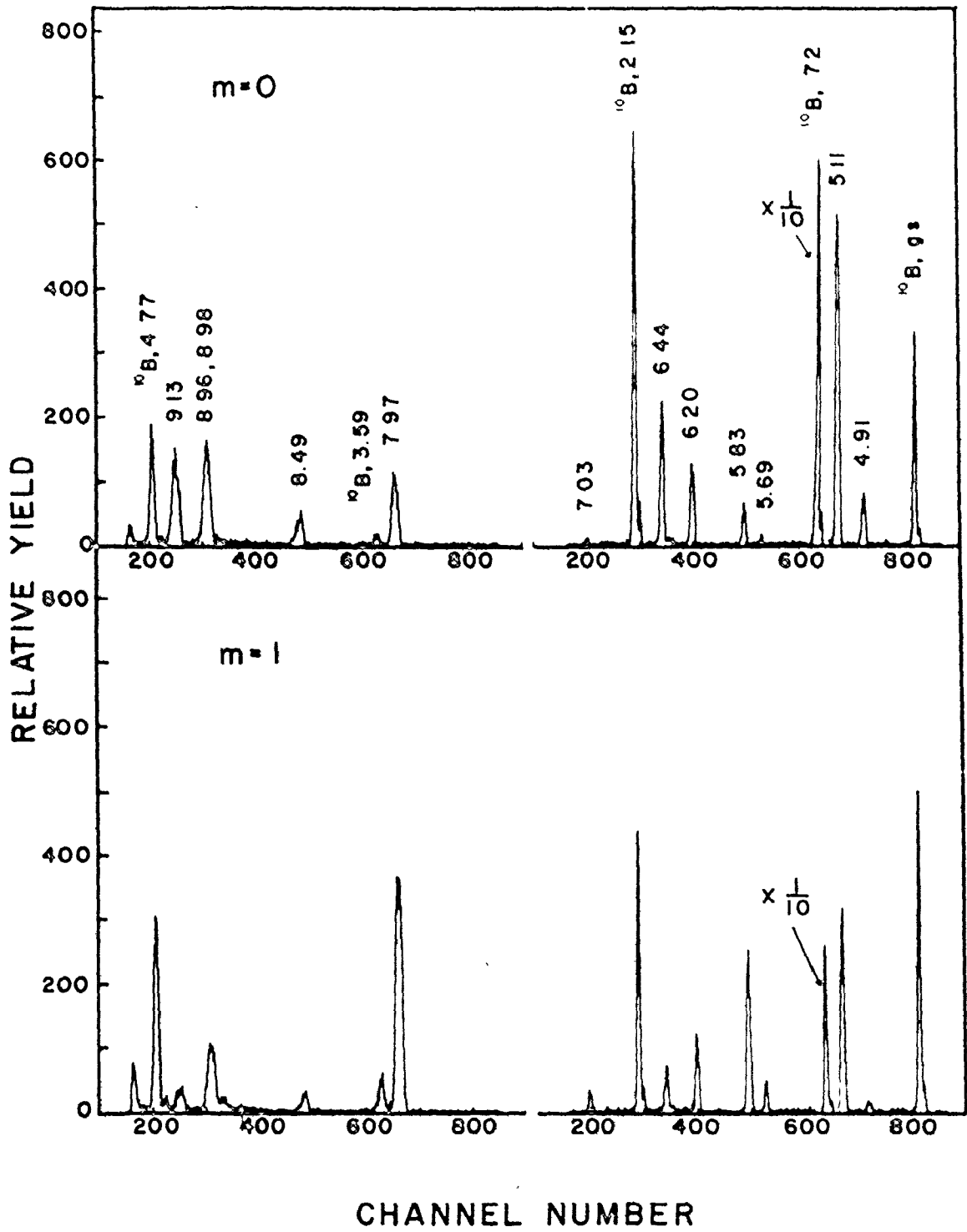
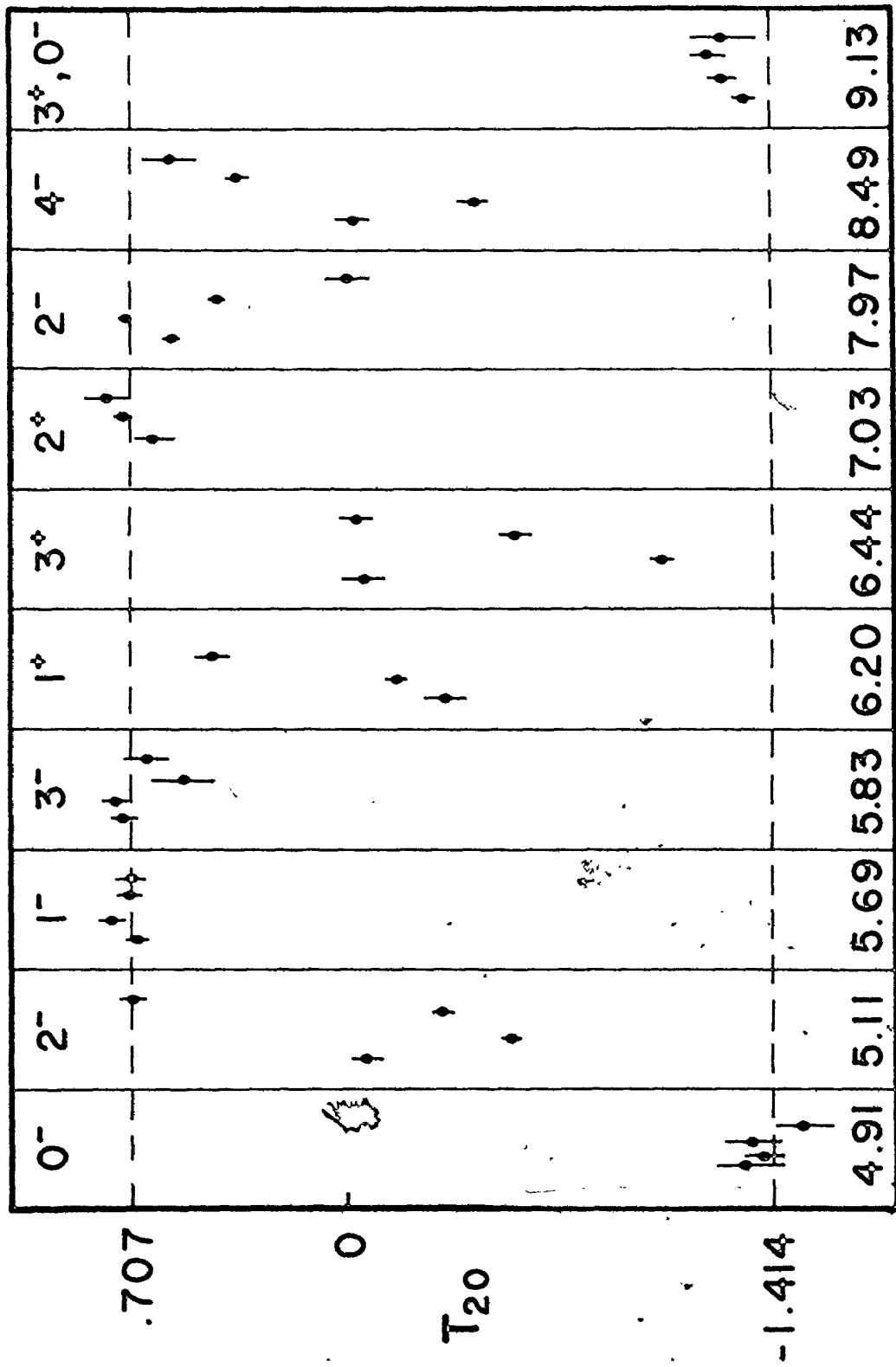


Figure 3.8

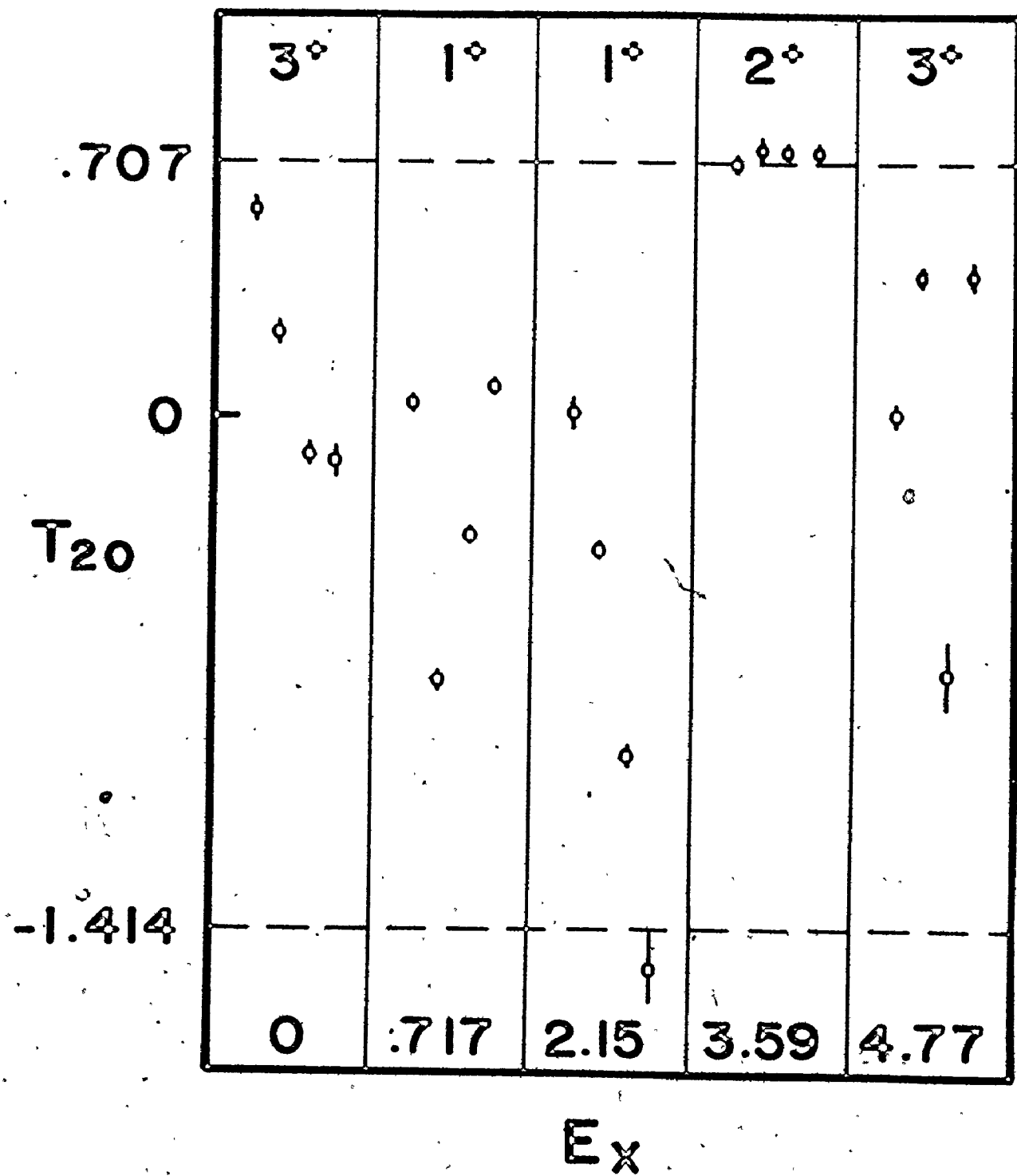
Tensor analyzing powers at  $\theta_{\text{lab}} = 2^\circ$  for states in  $^{14}\text{N}$  from the  $^{16}\text{O}(d,\alpha)^{14}\text{N}$  reaction. The data points, from left to right for each state, correspond to beam energies of 11, 12, 13, and 14 MeV, respectively. Only three measurements are available for the 6.20 and 7.03 MeV states, as noted in the text.



Ex

Figure 3.9

Tensor analyzing powers at  $\theta_{\text{lab}} = 2^\circ$  for states in  $^{10}\text{B}$  from  
the  $^{12}\text{C}(d,\alpha)^{10}\text{B}$  reaction.



ever, the difference involved is slight.

The statistical sample size for the data in this experiment is too small to make a definitive comparison with calculated distributions of the tensor analyzing power; however, it appears that the fluctuations of  $T_{20}$  for unnatural parity states are consistent with the calculations.

The results for the tensor analyzing powers of states in  $^{14}\text{N}$  from 4.91 to 9.13 MeV are consistent with all known spin-parity assignments. Isospin forbidden  $T = 1$  states were not observed in this reaction. The 6.20 MeV state was not observed at 14 MeV and the 7.03 MeV state was not observed at 11 MeV. An assignment of  $0^-$  to the state at 4.91 MeV confirms an earlier measurement made at this laboratory using the  $(d,\alpha)$  reaction (Jones et. al., 1975b). The states at 7.97, 8.49, and 9.13 MeV are discussed below.

(A) 7.97 MeV

This level has been assigned  $J^\pi = 2^-$  by Balamuth and Noé (1972) using model dependent arguments to rule out the possibilities of  $1^-$  and  $2^+$ . Our results show unambiguously that this is an unnatural parity state and thus confirm the assignment of  $J^\pi = 2^-$ .

(B) 8.49 MeV

This level has been assigned  $J^\pi = 4^-$  by Noé et. al. (1974) using model dependent arguments to rule out the possibility of  $4^+$ . Our results show unambiguously that this is an unnatural parity state and thus confirm the assignment of  $J^\pi = 4^-$ .

(C) 9.13 MeV

The 9.13 MeV level was observed by Detenbeck et. al (1965) as a weak resonance in the  $^{13}\text{C}(p,\gamma)^{14}\text{N}$  reaction and was assigned  $J^\pi = 2^-$  on the basis

of the  $\gamma$ -ray angular distribution. However, there is evidence that this state may actually be an unresolved doublet and Noé et. al. have concluded that one member might have  $J \geq 3$  in order to explain the proton angular correlation in the  $^{12}\text{C}(^3\text{He},p)^{14}\text{N}(p)^{13}\text{C}$  reaction. Fortune et. al. (1975) have found an  $L = 0$  component in the angular distribution of the  $^{10}\text{B}(^6\text{Li},d)^{14}\text{N}$  reaction and conclude that one member has  $J^\pi = 3^+$ . They suggest that this is the  $3^+$  state predicted by Lie (1972) but previously unidentified. Our results for the 9.13 MeV level show a  $T_{20}$  consistently very close to the limit for a  $0^-$  state, which strongly suggests that one member of the "doublet" has  $J^\pi = 0^-$ . Unidentified states having  $J^\pi = 0^-$ ,  $T = 0$  have been also predicted by Lie but at a somewhat higher excitation energy (13 MeV). One is tempted to conclude that the two members of the doublet have  $J^\pi = 3^+$  and  $J^\pi = 0^-$ .

## CHAPTER IV - The $^{40}\text{Ca}(d,\alpha)^{38}\text{K}$ Experiments

### Introduction

The nucleus  $^{38}\text{K}$  has been studied previously using the  $(d,\alpha)$  reaction, the  $(d,\alpha\gamma)$  reaction and also via particle transfer work, and as a result many low-lying positive parity states have been clearly identified and their  $\gamma$ -decay determined. However there exist many ambiguities with the negative parity states which makes comparison with shell model calculations especially difficult. This chapter reports measurements of the tensor analyzing power  $T_{20}$  at  $3^\circ$  for the  $^{40}\text{Ca}(d,\alpha)^{38}\text{K}$  reaction (Petty et. al., 1976b).

### Procedure

The experimental setup was substantially the same as discussed in the previous chapter. Alpha particle spectra were measured at  $3^\circ$  at beam energies of 7.5, 7.75, and 8.0 MeV. The target used was a  $25 \mu\text{g}/\text{cm}^2$  layer of natural Ca evaporated onto a  $10 \mu\text{g}/\text{cm}^2$  C backing. In order to minimize oxidation of the target, it was transferred to the target chamber in an argon atmosphere. For each beam energy, runs were carried out for deuterons polarized first in the  $m = 0$  substate ( $t_{20}(m = 0) = -P\sqrt{2}$ ), and second in the  $m = 1$  substate ( $t_{20}(m = 1) = P/\sqrt{2}$ ), where the quantization axis is taken parallel to the beam direction. The fractional beam polarization,  $P$ , was determined by measuring the tensor analyzing power for known natural parity states and a  $0^-$  state in  $^{38}\text{K}$ . It was found to be constant within about 10% during the 5 day run with an average value of 60%. In order to minimize the effect of long-term variations in the fractional beam polarization, the



deuteron substate was switched every 2 hours. Each run lasted for a total of about 8 hours with an average beam current of 30 nA.

The spectra for 8 MeV are plotted in Figure 4.1. States in  $^{38}\text{K}$  are labelled with their excitation energies and those arising from various impurities in the target are shown and labelled with the excitation energies. Excitation energies for states in  $^{38}\text{K}$  are taken from Collins et. al. (1975). It should be pointed out that the appearance of impurity peaks from  $^{13}\text{C}$  and  $^{24}\text{Mg}$  contaminants in the target is not too surprising since the cross-section for the (d, $\alpha$ ) reaction is much larger for these lower mass elements and therefore only a few percent of these impurities can account for the observed peaks. This also is the reason for observing the  $0^+$ , T = 1 state (2310keV) of  $^{14}\text{N}$  in the spectra; even the  $\sim 2\%$  yield allowed at  $3^\circ$  is enough to account for the observed intensity. The tensor analyzing powers at  $3^\circ$  for states in  $^{38}\text{K}$  from 1698 to 3978 keV are shown plotted in Figure 4.2 and Figure 4.3 The errors shown are based on the statistical uncertainty in determining the peak areas plus an estimated 5% error in measuring the beam polarizations.

### Results

Table 4.1 summarizes the results of this work showing the values of  $T_{20}$  which were calculated from the mean yields at 7.5, 7.75, and 8.0 MeV. States at 1698, 2647, 2870, 2992, 3317, 3342, 3458, 3815, 3841, 3857, 3934, and 3978 keV have been assigned unnatural parity while states at 2613 and 2828 keV have been assigned natural parity. The state at 2403 keV was observed only at 7.75 MeV and the state at 3615 keV was not observed at 7.5 MeV and only weakly excited at 7.75 and 8.0 MeV; in both cases the results are consistent with natural parity for these states. The results

Figure 4.1

Spectra for the  $^{40}\text{Ca}(\vec{d},\alpha)^{38}\text{K}$  reaction at  $E_d = 8$  MeV and  $\theta_{\text{lab}} = 3^\circ$ . The upper spectra are taken for the incident deuteron beam polarized in its  $m = 0$  substate and the lower spectra for the  $m = 1$  substate, where the quantization axis is aligned along the incident beam direction.

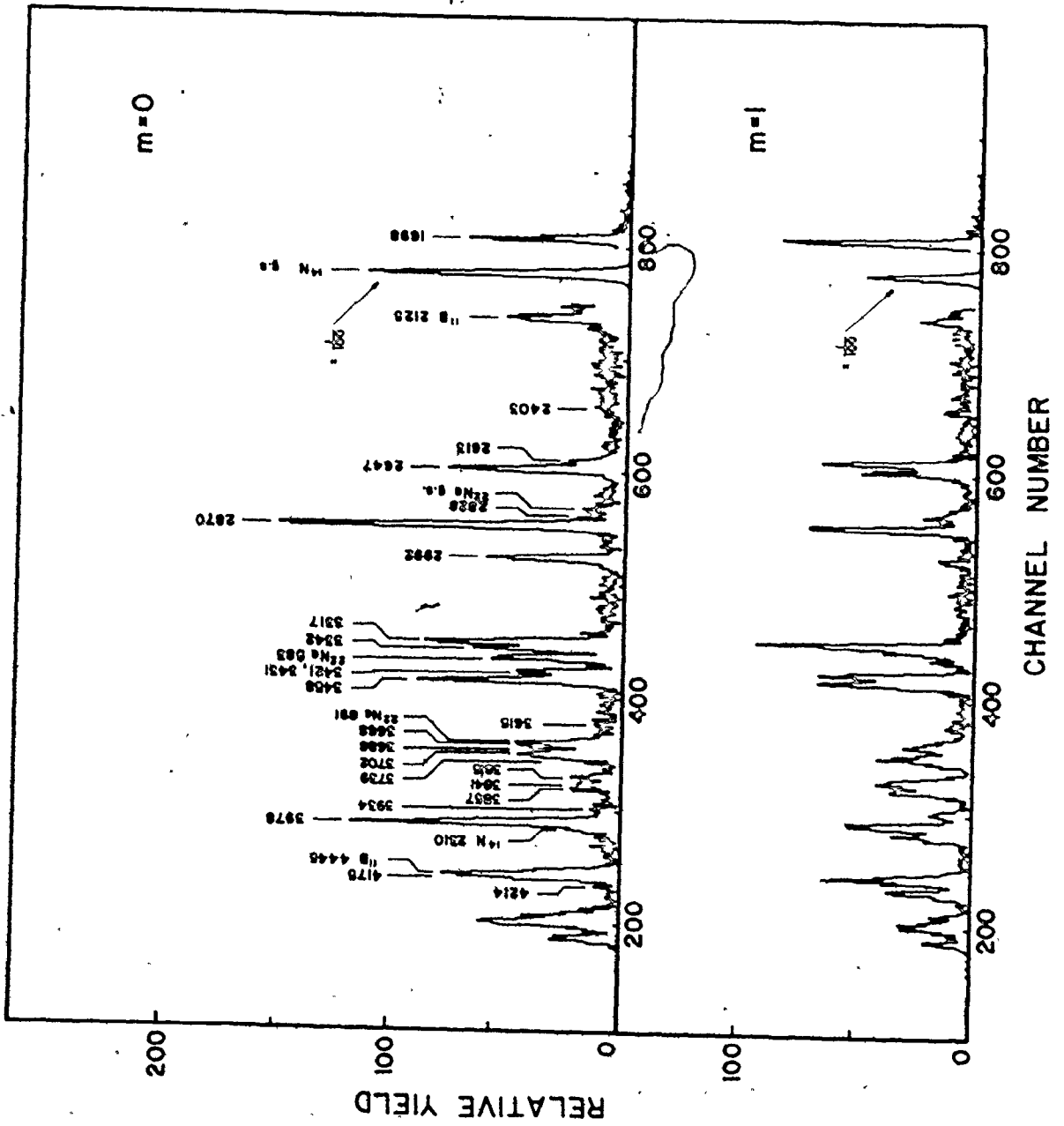
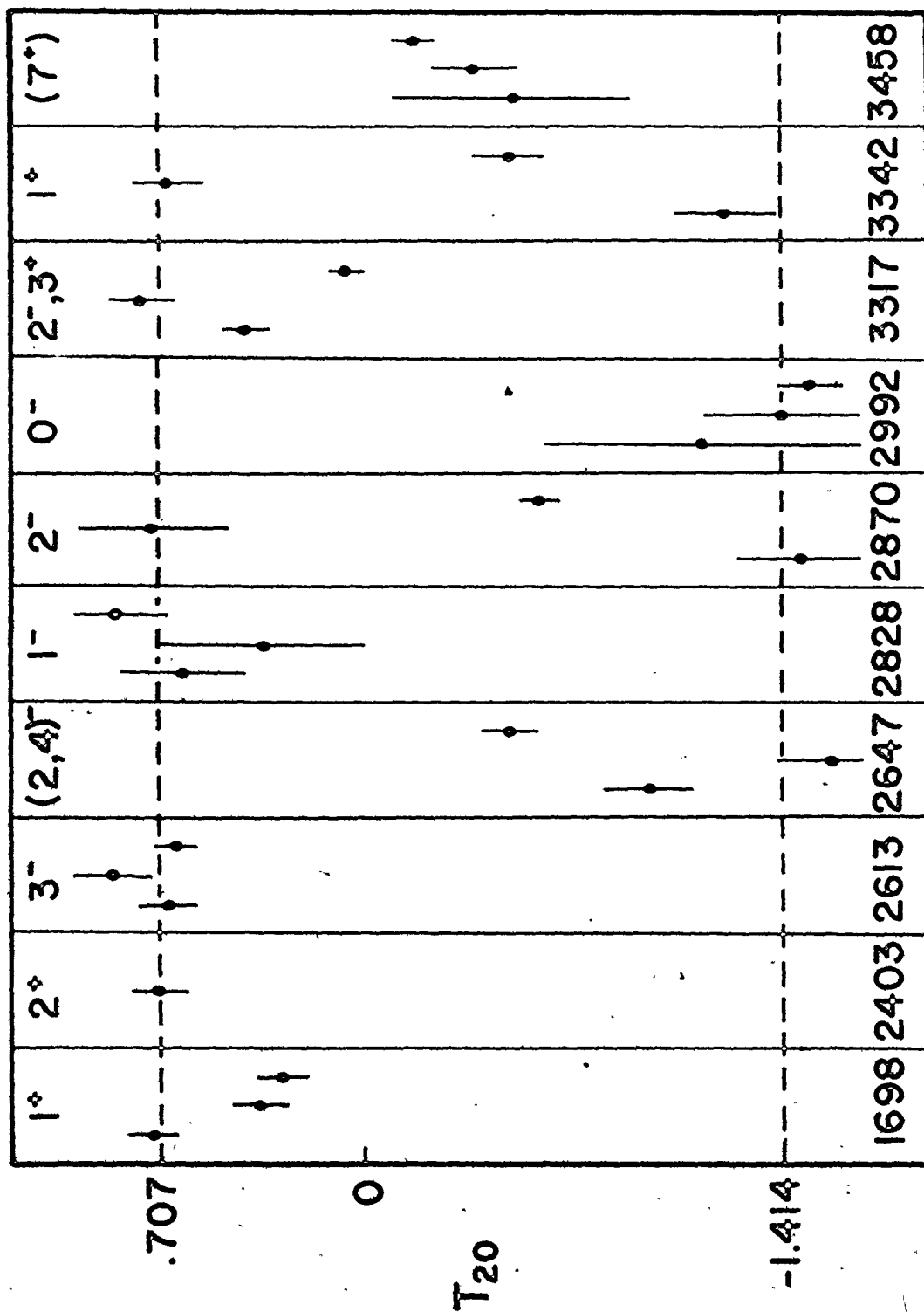


Figure 4.2

Tensor analyzing powers,  $T_{20}$ , at  $\theta_{\text{lab}} = 3^\circ$  for the  $^{40}\text{Ca}(d,\alpha)$  reaction for states in  $^{38}\text{K}$  from 1698 to 3458 keV. The data points, from left to right for each state, correspond to beam energies of 7.5, 7.75, and 8.0 MeV, respectively. Only one measurement is available for the 2403 keV state as noted in the text.



Ex

Figure 4.3

Tensor analyzing powers,  $T_{20}$ , at  $\theta_{\text{lab}} = 3^\circ$  for the  $^{40}\text{Ca}(d,\alpha)$  reaction for states in  $^{38}\text{K}$  from 3615 to 3978 keV. Only two measurements are available for the 3615 keV state, as noted in the text.

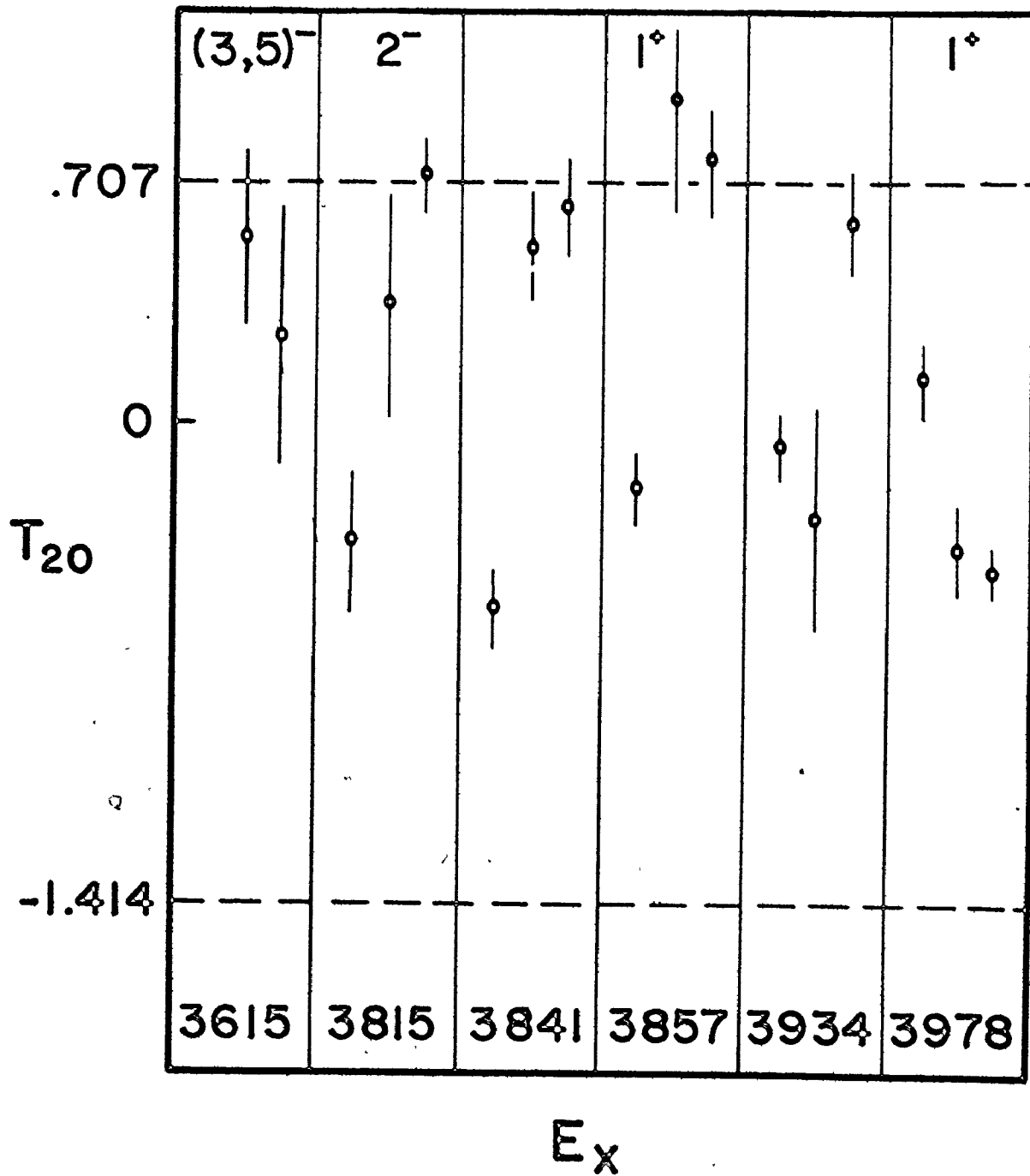


Table 4.1

Measured mean values of  $T_{20}$  ( $3^\circ$ ) for the  $^{40}\text{Ca}(d,\alpha)^{38}\text{K}$  reaction;  
Spectroscopic information for  $^{38}\text{K}$

$E_x$ a) (keV)	$J^\pi$ b)	$\langle T_{20} \rangle^c$	Parity <sup>d)</sup>	$J^\pi$ e)
0	$3^+$			
132	$0^+$			
459	$1^+$			
1698	$1^+$	$0.47 \pm .07$	U	A
2403	$2^+$	$0.69 \pm .09$	N	A
2613	$(2-4)^-$	$0.71 \pm .09$	N	$3^-$
2647	$(0-5)^-$	$-1.05 \pm .13$	U	$(2,4)^-$
2828	$1^-$	$0.52 \pm .20$	N	A
2870	$(1,2)^-$	$-0.58 \pm .11$	U	$2^-$
2992	$0^-$	$-1.35 \pm .22$	U	A
3317	$2,3^+$	$0.33 \pm .07$	U	$2^-, 3^+$
3342	$1^+$	$-0.28 \pm .10$	U	A
3421 } 3431 }	unresolved	$0.51 \pm .09$		
3458	$(7^+)$	$-0.27 \pm .10$	U	
3615	$(3,5)^-$	$0.41 \pm .27$	(N)	

(continued)



Table 4.1 (continued)

$E_x$	$J^\pi$	$\langle T_{20} \rangle$	Parity	$J^\pi$
3668	unresolved			
3688				
3702				
3739				
3815	$(0-3)^-$	$0.33 \pm .15$	U	$2^-$
3841		$-0.03 \pm .09$	U	
3857	$(1,2)^+$	$0.26 \pm .12$	U	$1^+$
3934		$0.14 \pm .12$	U	
3978	$(1,2)^+$	$-0.28 \pm .08$	U	$1^+$

- a) Excitation energies are taken from Collins et. al. (1975).
- b) Previous spin and parity assignments; see references quoted in text.
- c) Value of  $T_{20}$  calculated from mean yields for 7.5, 7.75, and 8.0 MeV, except where noted in text.
- d) U = unnatural; N = natural
- e) Assignments based partly on present work; "A" means agreement with previous results.

agree with the established spins and parities (Collins et. al., 1975, Endt and van der Leun, 1973; Wildenthal et. al., 1974; Hasper et. al., 1972; Hasper and Smith, 1973; Rickel et.al., 1976) for the states at 1698, 2403, 2828, 2992, 3342, and 3615 keV.

The present results allow new assignments or restrictions to be made to the states at 2613, 2647, 2870, 3317, 3815, 3857, and 3978 keV. Previous assignments of  $J^\pi = (1-3)$ ,  $(1-3)$  and  $(1,2)^+$  are listed in the compilation of Endt and van der Leun (1973) for the states at 2870, 3317, and 3978 keV. The state at 2992 keV has recently been assigned  $J^\pi = 0^-$  using the  $(d,\alpha)$  reaction near  $180^\circ$  (Rickel et. al., 1976). Wildenthal, Rice and Freedom (1974) have measured neutron pickup in the  $(p,d)$  reaction on  $^{39}\text{K}$  (g.s.  $J^\pi = 3/2^+$ ) and they report  $\ell = 3$  angular distributions for the 2613 and 2647 keV states, mixed  $\ell = 1 + 3$  angular distributions for the 2870 and 3815 keV states and mixed  $\ell = 0 + 2$  angular distributions for the 3857 and 3978 keV states. The  $\gamma$ -decay angular distributions of Hasper, Smith and Smulders (1972) and also of Collins et. al. (1975) and the lifetime measurements of Hasper and Smith (1973) can also be used to reduce the number of possible spin assignments to  $(2-4)^-$ ,  $(1,2)^-$  and  $2,3^+$  for the 2613, 2870, and 3317 keV states, respectively. Using the results of this work, unambiguous assignments of  $3^-$ ,  $2^-$ ,  $2^-$ ,  $1^+$  and  $1^+$  can be made to the states at 2613, 2870, 3815, 3857, and 3978 keV, respectively, and assignments restricted to  $(2,4)^-$  and  $(2^-,3^+)$  for the 2647 and 3317 keV states.

The doublet at 3421 and 3431 keV was not resolved, although the average value of  $T_{20}$  for both peaks is shown in the table. Since the value is not at the limit required for a natural parity level, it can be concluded only that the two states are not both natural parity. No attempt was made

to fit the group of states 3668, 3688, 3702, and 3739 keV (including one impurity peak) since it was felt that they were not sufficiently resolved to yield reliable information. The three states at 3815, 3841, and 3857 keV were also not well resolved; however a good fit was obtained for them using gaussian peaks of equal width plus a linear background. The positions of the peaks were fixed at locations predicted by an energy calibration of the focal plane detector.

Recently there has been some interest (van Driel et. al., 1974; Yates et. al., 1974) in two possible high-spin states of  $6^-$  and  $7^+$  at 3421 and 3458 keV, respectively. It is only possible to say, however, that the results of the present <sup>□</sup> work do not disagree with their suggestions.

## CHAPTER V - Shell Model Calculations for $^{38}\text{K}$

### Introduction

The low-lying positive parity states in the nucleus  $^{38}\text{K}$  have been studied theoretically by several groups with varying results. In general, there is good agreement with experiment for the energies of these states although discrepancies exist for the beta decay rates and electromagnetic lifetimes since these properties are more sensitive to small admixtures in the wavefunctions. There have been many fewer calculations done for the negative parity states, however. This is for two reasons:

- (i) The larger model space required for negative parity states gives rise to considerable computational difficulties, and;
- (ii) Until recently, the lack of experimental data has prevented a realistic comparison with the theory.

In this chapter we present the results of shell-model calculations for the  $T = 0$  negative parity states in  $^{38}\text{K}$ .

### Details of the Calculation

Figure 5.1 shows the experimental spectrum of two mass-38 isobars, Ar and K. The  $0^+$  and  $2^+$   $T = 1$  states have been identified in  $^{38}\text{K}$  although as yet the analog for the second  $0^+$  state in Ar has not been identified. It is clear from this figure that a calculation on the  $T = 0$  negative parity levels will be necessary for an understanding of the new experimental data in  $^{38}\text{K}$ .

$^{38}\text{K}$  has 19 protons and 19 neutrons and, in the simple independent particle model, low-lying positive parity states should be represented by

Figure 5.1

Level diagrams for  $^{38}\text{Ar}$  and  $^{38}\text{K}$ . The  $^{38}\text{Ar}$  spectra are included as an aid in the identification of  $T = 1$  states in  $^{38}\text{K}$ .



two holes in the  $1d_{3/2}$  orbit. Figure 5.2 shows the shell structure in this mass region where  $^{40}\text{Ca}$  is considered to be a closed shell nucleus. Next higher configurations would include particle excitations from the  $1d_{5/2}$  and  $2s_{1/2}$  orbits schematically represented by  $(d_{5/2}s_{1/2}d_{3/2})^{-2}$  or simply  $(sd)^{-2}$ . Wildenthal et.al. (1971) have done calculations in the full sd-shell model space using several different interactions and conclude that, while the ground state wavefunction of  $^{38}\text{K}$  has a >90%  $(d_{3/2})^{-2}$  configuration the other positive parity states have less than 50%  $(d_{3/2})^{-2}$ . In all cases however, the  $d_{5/2}$  orbit seems to be unimportant. Evers and Stocker (1970) have included configurations involving two particles in the  $1f_{7/2}$  shell {i.e.  $(s_{1/2}d_{3/2})^{-4}(f_{7/2})^2$ } and find that these may account for as much as 40% of the wavefunctions for the two lowest  $1^+$  states. To a first approximation, the low-lying negative parity states should be described by promoting 1 particle into the  $1f_{7/2}$  orbit {i.e.  $(d_{3/2})^{-3}(f_{7/2})^1$ } and calculations of this type have been carried out by Ern  (1966), while calculations involving the  $2p_{3/2}$  orbit have been carried out by Engelbertink and Glaudemans (1969). For the calculation presented in this chapter, two model spaces were chosen:

- (i)  $(d_{3/2})^{-3} (f_{7/2}p_{3/2})^1$
- (ii)  $(s_{1/2}d_{3/2})^{-3} (f_{7/2}p_{3/2})^1$

Choice (i) is the one used by Engelbertink and Glaudemans while the choice of number (ii) is suggested by the results of the calculation by Wildenthal et. al. Unfortunately, computational restrictions prevented the inclusion of configurations like  $(s_{1/2}d_{3/2})^{-5}(f_{7/2}p_{3/2})^3$ , which are probably important.

There are three approaches in determining the residual interaction

Figure 5.2

Shell structure around  $^{38}\text{K}$ . The single particle energies of the orbits are the ones used in the shell-model calculation.  $^{40}\text{Ca}$  is here depicted as a closed shell with all of the orbits up to and including the  $1d_{3/2}$  orbit full.



Single Particle Energy (MeV)



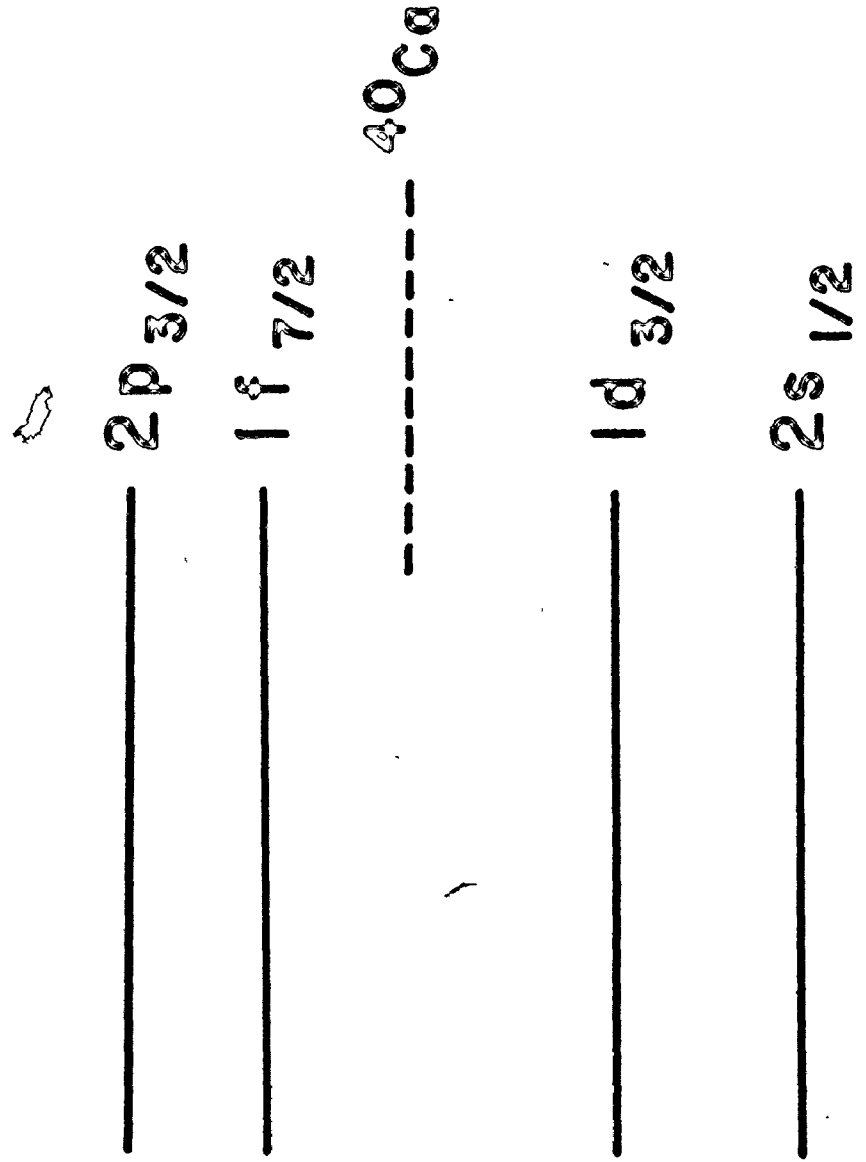
$2p_{3/2}$

$1f_{7/2}$

40Ca

$1d_{3/2}$

$2s_{1/2}$



to use in calculations of this type:

- (i) The values of the matrix elements can be determined by a fit to the known levels of several nearby nuclei. Depending on the model space chosen, the number of matrix elements can quickly surpass the known number of levels, however. Ern  fitted the 14 one- and two-body matrix elements appropriate to the  $(d_{3/2})^{-3}(f_{7/2})^1$  space to 60 binding and excitation energies in the region  $A = 33 - 41$ .
- (ii) A so-called "realistic" interaction may be used. In this case the matrix elements are obtained by fitting the parameters of some nuclear potential to the free nucleon-nucleon scattering data. An example of this approach may be found in the work of Dieperink and Brussaard (1969) who used the Tabakin interaction to calculate positive parity states in the mass region  $36 < A < 39$ . It should be pointed out that satisfactory agreement for  $^{38}\text{K}$  could only be obtained if the interaction was modified slightly for that nucleus.
- (iii) A phenomenological interaction may be used. An interaction of this type will have some parameters, such as its strength, which are adjusted to give the best fit to the experimental data. Engelbertink and Glaudemans have used the modified surface delta interaction (MSDI) in their calculation of the low-lying negative parity states for  $A = 38$  nuclei.

It was decided to use the MSDI for these calculations partly because of its fairly simple form and partly because of its past successes in shell model calculations (Glaudemans et. al., 1967; Engelbertink and Glaudemans,

1969; and Maripuu and Hokken, 1970). The modified surface delta interaction is defined as (Glaudemans et. al., 1967)

$$V_{ij} = -4\pi A_T \delta(R-r_i) \delta(R-r_j) \delta(\Omega_{ij}) + B_T$$

The four strength parameters,  $A_0$  and  $B_0$  for a  $T = 0$  coupled pair and  $A_1$  and  $B_1$  for a  $T = 1$  coupled pair are the only free parameters to be adjusted in the expressions for the two-body matrix elements. The parameters  $B_0$  and  $B_1$  give the binding energy and the relative spacing between states with different isospin and will not affect these calculations since we are only interested in the relative spacing of the  $T = 0$  negative parity states.

The values of the one-body matrix elements (i.e. the single particle energies) can be determined by examining the spectroscopic information for nuclei such as  $^{39}\text{Ca}$  and  $^{39}\text{K}$  etc. Since the single particle strength is usually spread out over several states, it is often necessary to take a weighted average of these values.

### Results

The single particle energies used are taken from Grawe et. al. (1974) and the initial values of the MSDI parameters are taken from Engelbertink and Glaudemans (1969). These are listed in Table 5.1. Only the values of the MSDI parameters  $A_0$  and  $A_1$  and the energy differences  $\epsilon(s_{1/2}) - \epsilon(d_{3/2})$  and  $\epsilon(p_{3/2}) - \epsilon(f_{7/2})$  affect the calculations. All calculations were done using the Oak Ridge-Rochester shell model code (Wong, 1966; French et. al. 1969) which ran on the McMaster CDC 6400 computer. Typical size of the energy matrices was  $20 \times 20$ . The results of the calculations are shown in Figure 5.3. Two points are worth mentioning. First, the results for many of the states do not change appreciably when excitations are allowed

Table 5.1

Parameters used in shell-model calculation

## (a) MSDI parameters (MeV)

$$A_0 = 0.69$$

$$A_1 = 1.15$$

$$B_0 = -1.44$$

$$B_1 = 0.66$$

## (b) Single particle energies (MeV)

$$\epsilon(s_{1/2}) = -9.65$$

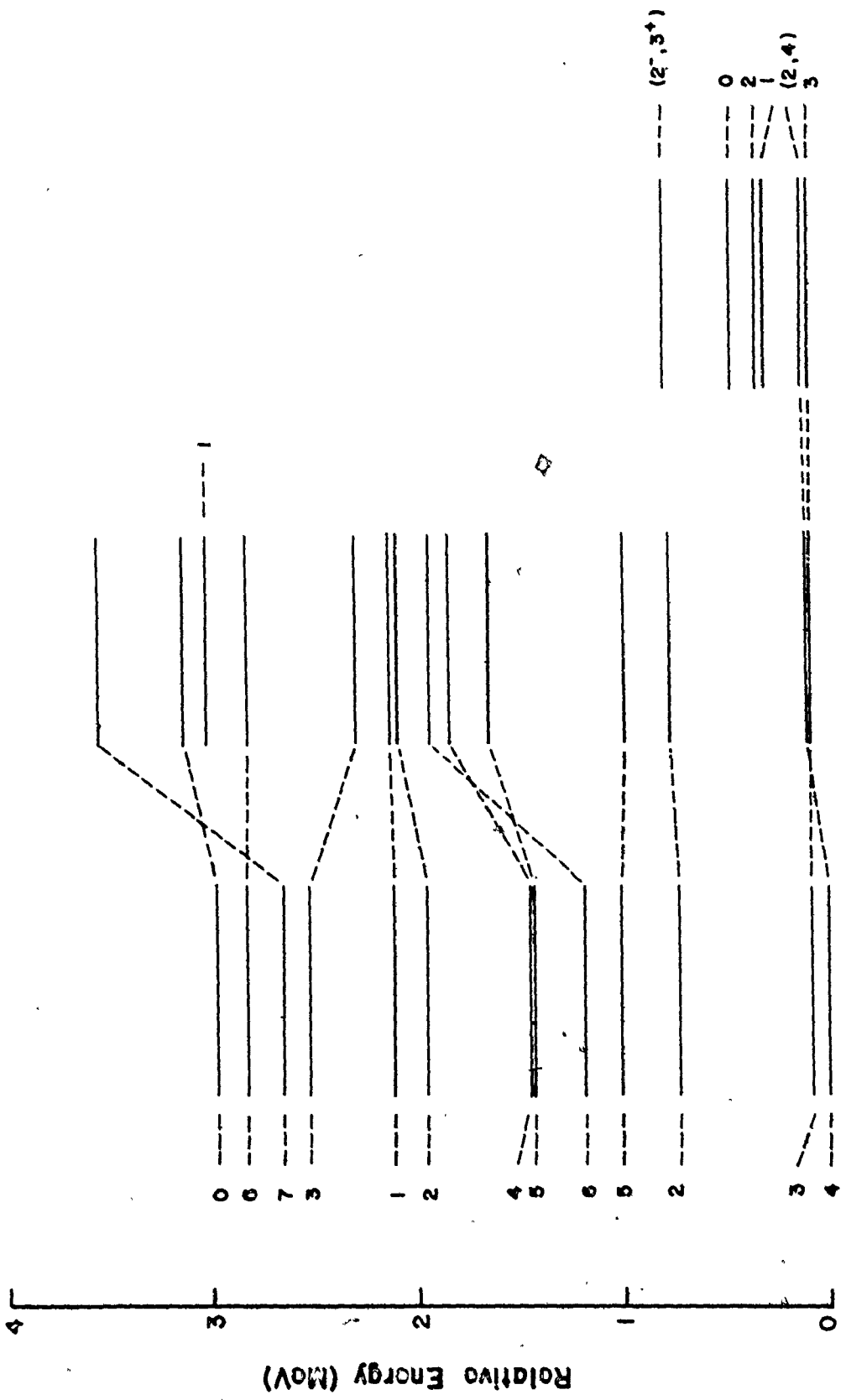
$$\epsilon(d_{3/2}) = -7.55$$

$$\epsilon(f_{7/2}) = -3.50$$

$$\epsilon(p_{3/2}) = -1.90$$

Figure 5.3

Results of a shell-model calculation for the  $T = 0$  negative parity states in  $^{38}\text{K}$ . The labels under the level diagrams indicate the model space used in the calculations, with the relevant portion of the experimental level diagram shown on the right.



from the  $s_{1/2}$  orbit. Second, there is relatively poor agreement for most of the states except the lowest two.

In order to determine how sensitive the calculated energies are to the values of the parameters  $A_0$  and  $A_1$ , a series of calculations was performed. The results are shown in Figures 5.4 and 5.5. In each case the value of one parameter was held constant and the other varied over a region around its original value. It is clear that no significant improvement can be obtained unless possibly extreme values are used. Since the initial values for the parameters are similar to ones found to give best fits for other nuclei in this mass region, other explanations for the disagreement must be offered.

Table 5.2 shows the dominant configurations present in the lowest four calculated negative parity states. There is good agreement for the energies of the  $3^-$  and  $4^-$  states (at 2613 and 2647 keV, relative to the ground state) which are mostly  $(d_{3/2})^{-3}(f_{7/2})^1$ , but relatively poor agreement for the other states. This is probably due to the need for including a larger configuration model space in the calculations.

In conclusion, the results of the calculations presented in this chapter indicate that the state at 2647 keV in  $^{38}\text{K}$  is most likely a  $4^-$  state (rather than  $2^-$ ) but predictions for other states are not possible at this time. The need to include a larger configuration space in the calculations probably reflects the fact that  $^{40}\text{Ca}$  is not really a good closed-shell nucleus and that "core" excitations must be taken into account when considering negative parity states above 2647 keV.

Figure 5.4

Relative energies of low-lying negative parity states as a function of the MSDI parameter  $A_0$ . Only the lowest two states (below 4 MeV) for each spin are shown and therefore the level density may be misleading.



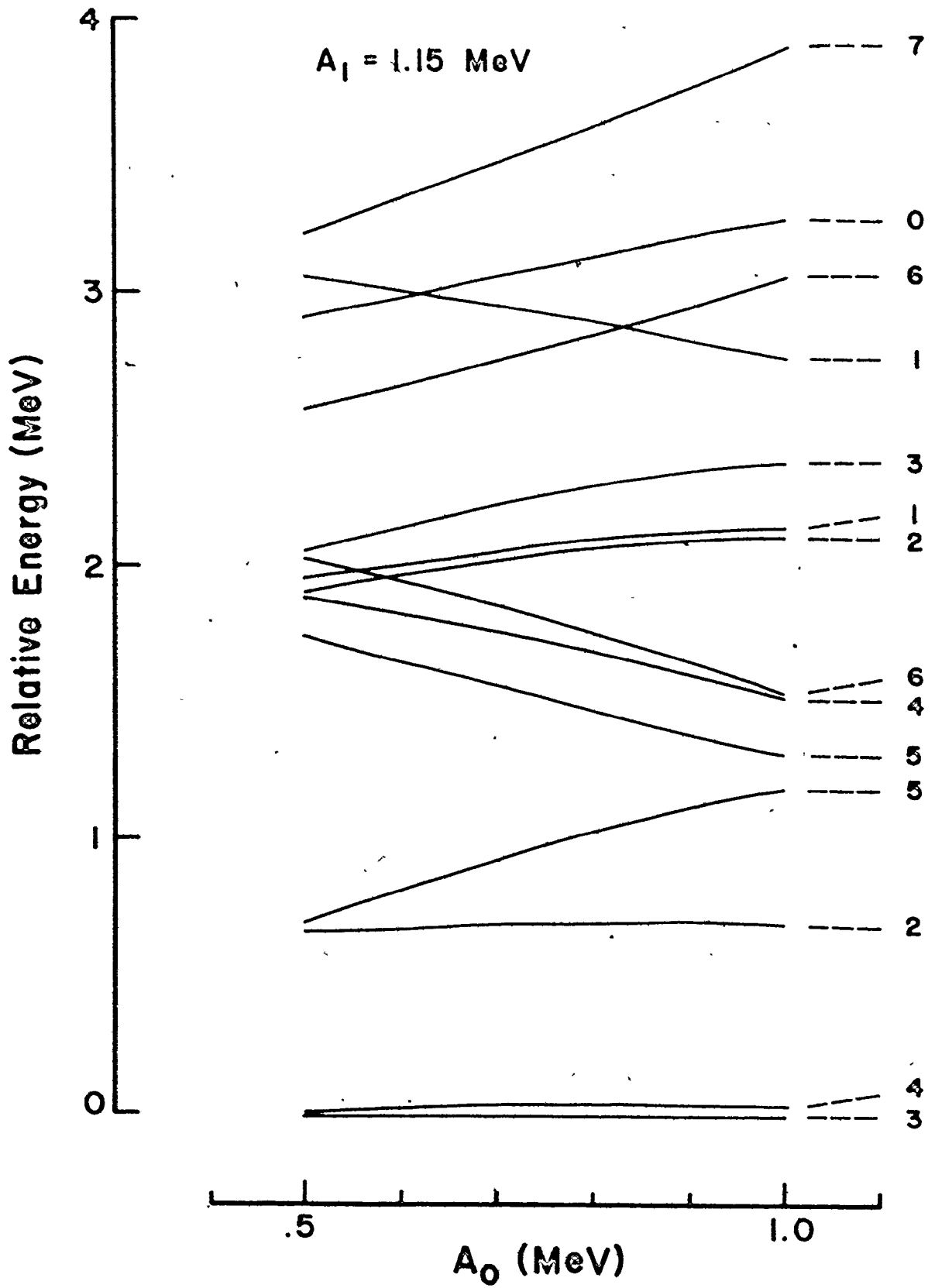


Figure 5.5

Relative energies of low-lying negative parity states as a function of the MSDI parameter  $A_1$ .

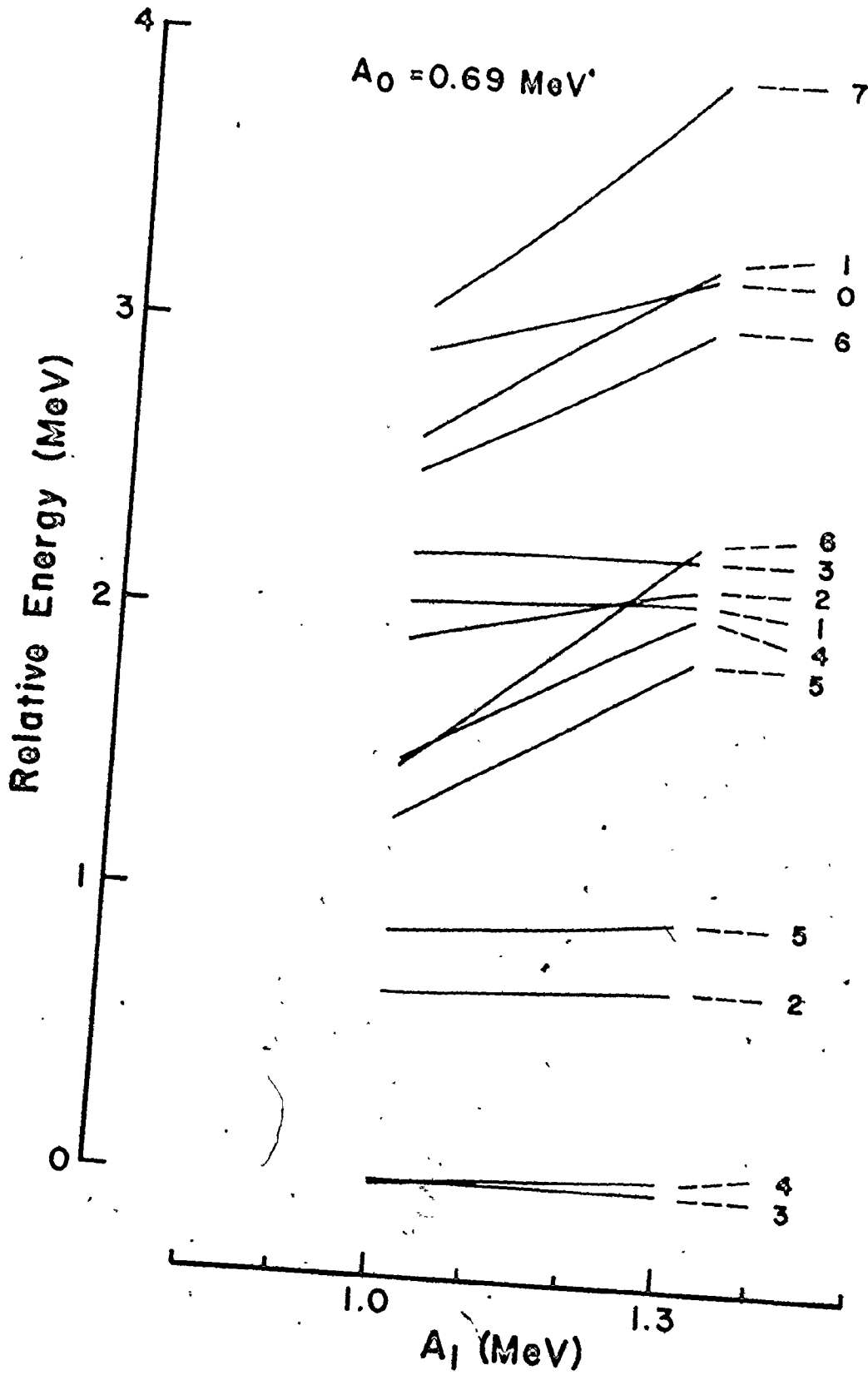


Table 5.2

Dominant configurations in some low-lying negative parity states

Energy <sup>a)</sup> (MeV)	J <sup>π</sup>	Configuration (particles/shell)				Contribution <sup>b)</sup>
		s <sub>1/2</sub>	d <sub>3/2</sub>	f <sub>7/2</sub>	p <sub>3/2</sub>	
0.0	3 <sup>-</sup>	4	5	1	0	74%
		4	5	0	1	8%
		2	7	1	0	8%
0.022	4 <sup>-</sup>	4	5	1	0	84%
		2	7	1	0	8%
0.687	2 <sup>-</sup>	4	5	1	0	54%
		4	5	0	1	29%
		2	7	1	0	5%
0.910	5 <sup>-</sup>	4	5	1	0	80%
		2	7	1	0	9%

a) Energy relative to the lowest 3<sup>-</sup> state.

b) Amplitude squared.

## CONCLUSIONS

It has been shown that the polarized ( $\vec{d}, \alpha$ ) reaction near  $0^\circ$  on an even-even target nucleus is a useful model-independent technique for determining spin and/or parity assignments in the residual odd-odd nuclei. The effect of detecting the alpha particles slightly off-axis has been studied and it was found that  $2^\circ$  is close enough to  $0^\circ$  to be useful but that, in some cases,  $5^\circ$  may not be. In addition it was found that measurements taken at three different beam energies would usually be sufficient to average out effects of the so-called Ericson fluctuations in the reaction amplitudes.

In this thesis, the method has been applied to states in  $^{10}\text{B}$ ,  $^{14}\text{N}$ , and  $^{38}\text{K}$  and several new spin and parity assignments have been made. Additional measurements on other states in these nuclei will only be possible when detection systems are available with improved energy resolution. Such a system is already under development at McMaster (Wilkin, 1976) and plans for its future use are being made.

The results of a shell-model calculation for the negative parity  $T = 0$  states in  $^{38}\text{K}$  are not too encouraging. Except for the lowest two states, it is apparent that one must include a larger configuration model-space in the calculations. Although this poses considerable computational difficulties, at least one group is now attempting such calculations (Hasper, 1974).

The advantages of using polarized beams in nuclear reaction studies have been alluded to in the Introduction and, of course, they are a cen-

tral requirement in this method. Beyond this, the method can be extended to include studying the  $\gamma$ -ray decay of the excited states in the final nucleus. By using a polarized beam, the relative population of various magnetic substates of the final state can be varied, thus changing the resulting radiation pattern observed. In this way it is often possible to remove spin ambiguities which otherwise might be present (Jones et. al., 1975a; Kuehner et. al., 1976). Work of this nature is now just starting at McMaster and it is expected to play a major role in the group's future activities. The combination of the results from the  $(\vec{d},\alpha)$  and the  $(\vec{d},\alpha\gamma)$  experiments form a powerful spectroscopic tool for the physicist to use in his study of the nucleus.

## REFERENCES

- F. Ajzenberg-Selove, Nucl. Phys. A. (to be published) 1976.
- F. Ajzenberg-Selove and T. Lauritsen, Nucl. Phys. A227, 1 (1974).
- D.P. Balamuth and J.W. Noé, Phys. Rev. C6, 30 (1972).
- J.M. Blatt and V.F. Weisskopf. Theoretical Nuclear Physics. (Wiley, New York, 1952).
- D.O. Boerma, W. Grüebler, V. König, P.A. Schmelzbach, and R. Risler, Nucl. Phys. A255, 275 (1975).
- D.M. Brink and R.O. Stephen, Phys. Lett. 5, 77 (1963).
- W.K. Collins, D.S. Longo, J.F. Mateja, P.R. Chagnon, E.D. Berners, G.F. Neal, C.P. Browne, P.L. Jolivet, A.A. Rollefson, and J.D. Goss, Phys. Rev. C11, 1925 (1975).
- S.E. Darden, Am. J. Phys. 35, 727 (1967).
- S. E. Darden in Polarization Phenomena in Nuclear Reactions, ed. H.H. Barschall and W. Haerberli (University of Wisconsin Press, Madison, 1971) p. 39.
- R.W. Deenbeck, J.C. Armstrong, A.S. Figuera, and J.B. Marion, Nucl. Phys. 8, 552 (1965).
- A.E.L. Dieperink and P.J. Brussaard, Nucl. Phys. A128, 34 (1969).
- P.M. Endt and C. van der Leun, Nucl. Phys. A214, 1 (1973).
- G.A.P. Engelbertink and P.W.M. Glaudemans, Nucl. Phys. A123, 225 (1969).
- J.B.A. England. Techniques in Nuclear Structure Physics, 2 vols. (Wiley, Toronto, 1974).
- T. Ericson, Nucl. Phys. 17, 250 (1960).
- T. Ericson, Phys. Lett. 4, 258 (1963).
- F.C. Ern , Nucl. Phys. 84, 91 (1966).

- D. Evers and W. Stockev, Phys. Lett. 33B, 559 (1970).
- H. Feshbach in Nuclear Spectroscopy, part B, ed. F. Ajzenberg-Selove (Academic, New York, 1960) p. 662.
- P.D. Forsyth A.R. Knudson, and F.C. Young, Nucl. Phys. 85, 153 (1966).
- H.T. Fortune, H.G. Bingham, D.J. Crozier, and J.N. Bishop, Phys. Rev. C11, 302 (1975).
- J.B. French, E.C. Halbert, J.B. McGrory, and S.S.M. Wong, in Advances in Nuclear Physics, vol. III, ed. M. Baranger and E. Vogt. (Plenum, New York, 1969) p. 193.
- C. Froberg, Rev. Mod. Phys. 27, 399 (1955).
- H.W. Fulbright, R.G. Markham, and W.A. Lanford, Nucl. Instr. Meth. 108, 125 (1973).
- P.W.M. Glaudemans, P.J. Brussaard, and B.H. Wildenthal, Nucl. Phys. A102, 593 (1967).
- N.B. Gove and R.L. Robinson, eds. Nuclear Spin-Parity Assignments. (Academic, New York, 1966).
- H. Grawe, J.E. Cairns, M.W. Greene, and J.A. Kuehner, Can. J. Phys. 52, 950 (1974).
- H. Hasper, PhD thesis, University of Groningen, 1974.
- H. Hasper and P.B. Smith, Phys. Rev. C8, 2240 (1973).
- H. Hasper, P.B. Smith, and P.J.M. Smulders, Phys. Rev. C5, 1261 (1972).
- W. Hauser and H. Feshbach, Phys. Rev. 87, 366 (1952).
- M. Jacob and G.C. Wick, Ann. Phys. 7, 404 (1959).
- J. Jänecke, Nucl. Phys. 48, 129 (1963).
- G.D. Jones, P.W. Green, J.A. Kuehner, and D.T. Petty, Nucl. Instr. Meth. 129, 527 (1975a).
- G.D. Jones, P.W. Green, J.A. Kuehner, D.T. Petty, J. Szücs, and H.R. Weller, Phys. Lett. 59B, 236 (1975b).
- J.A. Kuehner, P.W. Green, G.D. Jones, and D.T. Petty, Phys. Rev. Lett. 35, 423 (1975).



- J.A. Kuehner, J. Szűcs, P. Ikossi, A. McDonald and D.T. Petty,  
Phys. Rev. Lett. (to be published, 1976).
- W. Lakin, Phys. Rev. 98, 139 (1955).
- S. Lie, Nucl. Phys. A181, 517 (1972).
- S. Maripuu and G.A. Hokken, Nucl. Phys. A141, 481 (1970).
- J.W. McKay, MSc thesis, McMaster University, 1976.
- V. Meyer, R.E. Pixley, and P. Trüol, Nucl. Phys. A101, 321 (1967).
- J.W. Noé, E.P. Balamuth, and R.W. Zurmühle, Phys. Rev. C9, 132 (1974).
- G.G. Ohlsen, "Los Alamos Lamb-Shift Polarized Ion Source: A User's Guide",  
Los Alamos Scientific Laboratory Report LA-4451 (1970).
- D.T. Petty, "User's Guide to the Position Sensitive Proportional Counter",  
McMaster University Tandem Accelerator Laboratory Internal Report  
(unpublished, 1974).
- D.T. Petty, J.A. Kuehner, J. Szűcs, P.W. Green, and G.D. Jones, Phys. Rev.  
C14, 12 (1976a).
- D.T. Petty, P.G. Ikossi, J.A. Kuehner, and J. Szűcs, Phys. Rev.  
C14, 908 (1976).
- D.G. Rickel, N.R. Roberson, J.D. Turner, H.R. Weller, and D.R. Tilley,  
Phys. Rev. C13, 2077 (1976).
- E. Segré, ed. Experimental Nuclear Physics, 3 vols. (Wiley, Toronto, 1953).
- A.J. Sierk and T.A. Tonbrello, Nucl. Phys. A210, 341 (1973).
- M. Simonius, in Polarization Nuclear Physics, ed. D. Fick. (Springer-  
Verlag, New York, 1974) p. 38.
- M.A. van Driel, H.H. Eggenhuisen, J.A.J. Hermans, D. Bucurescu,  
H.A. van Rinsvelt, and G.A.P. Engelbertink, Nucl. Phys. A226, 326, (1974).
- T.A. Welton, in Fast Neutron Physics, vol II, ed. J.B. Marion and J.L. Fowler.  
(Interscience, New York, 1963) p. 1317.
- B.H. Wildenthal, E.C. Halbert, J.B. McGrory, and T.T.S. Kuo, Phys. Rev.  
C4, 1266, (1971).
- B.H. Wildenthal, J.A. Rice, and B.M. Freedom, Phys. Rev. C10, 2184 (1974).

G.B. Wilkin, MSc. project thesis, McMaster University, 1976.

S.S.M. Wong, PhD. thesis, University of Rochester, 1966.

S.W. Yates, F.J. Lynch, R.E. Holland, I. Ahmad, and A.M. Friedman,  
Phys. Rev. C9, 1857 (1974).

## APPENDIX I

## Papers published while working at McMaster

1. "A New Technique for Parity Measurement Using Polarized Deuterons" •  
J. A. Kuehner, P. W. Green, G. D. Jones and D. T. Petty,  
Physical Review Letters 35, 423 (1975).
2. " $\gamma$ -ray Decay of the 9.042 and 9.806 MeV States in  $^{23}\text{Na}$ "  
P. W. Green, G. D. Jones, D. T. Kelly, J. A. Kuehner and  
D. T. Petty, Physical Review C12, 887 (1975).
3. "Identification of  $J^\pi = 0^-$  Levels in Odd-Odd Nuclei and the  
Absolute Determination of  $t_{20}$  for Polarized Spin-1 Beams"  
G. D. Jones, P. W. Green, J. A. Kuehner, D. T. Petty, J. Szücs  
and H. R. Weller, Physics Letters 59B, 236 (1975).
4. "Nuclear Spectroscopy Using  $(d,\alpha\gamma)$  Angular Correlations"  
G. D. Jones, P. W. Green, J. A. Kuehner and D. T. Petty,  
Nuclear Instruments and Methods 129, 527 (1975).
5. "Elastic Scattering of Polarized Protons from  $^{56}\text{Fe}$  in the Giant  
Resonance Region of  $^{57}\text{Co}$ "  
H. R. Weller, J. Szücs, J. A. Kuehner, G. D. Jones and D. T. Petty,  
Physical Review C13, 1055 (1976).
6. "Tensor Analyzing Power Measurements in the  $^{16}\text{O}(\vec{d},\alpha)^{14}\text{N}$  Reaction at  $0^\circ$ "  
D. T. Petty, J. A. Kuehner, J. Szücs, P. W. Green and G. D. Jones,  
Physical Review C14, 12 (1976).
7. "Spin and Parity Assignments in  $^{38}\text{K}$  via the  $(\vec{d},\alpha)$  Reaction near  $0^\circ$ "  
D. T. Petty, P. G. Ikossi, J. A. Kuehner and J. Szücs,  
Physical Review C (to be published in September 1976 issue).
8. "Use of Tensor Polarized Deuterons in Method II Angular Correlations"  
J. A. Kuehner, J. Szücs, P. Ikossi, A. McDonald and D. T. Petty,  
Physical Review Letters (to be published).